

Critical Properties of 1-D Spin 1/2 Antiferromagnetic Heisenberg Model

J.F. Audet¹, A. Fledderjohann², C. Gerhardt², M. Karbach², H. Kröger^{1*}, K.H. Mütter² and M. Schmidt²

¹ Département de Physique, Université Laval, Québec, Québec, G1K 7P4, Canada
Email: hkroger@phy.ulaval.ca

² Physics Department, University of Wuppertal, D-42097 Wuppertal, Germany

Abstract. We discuss numerical results for the $1 - D$ spin 1/2 antiferromagnetic Heisenberg model with next-to-nearest neighbour coupling and in the presence of an uniform magnetic field. The model develops zero frequency excitations at field dependent soft mode momenta. We compute critical quantities from finite size dependence of static structure factors.

1 Introduction

The study of quantum spin systems in one space dimension (spin chain) can be motivated as follows: There are models which are exactly soluble, e.g., the Heisenberg model. "Exact" numerical results can be obtained by diagonalization of the Hamiltonian for reasonably large chains (up to approximately 50 spins). These quite precise data allow to carry out a finite size analysis and extrapolate to the thermodynamic limit. On the other hand, $1 - D$ spin chains have been analyzed by different techniques, like quantum Monte Carlo methods, coupled cluster method (*exp(S)*-method), renormalization group techniques etc., and thus constitute a benchmark problem for comparison of various methods. From the physics point of view, there are substances occurring in nature having predominantly the structure of a $1 - D$ chain. Examples are $CuCl_2 2NC_5H_5$ or $Cu(NH_3)_4SO_4 H_2O$ (Mazzi 1955), (Dunitz 1957), (Bernasconi 1981). New neutron scattering experiments on the quasi 1-D antiferromagnet $KCuF_3$ are discussed by Tennant et al. (Tennant 1995). There are recent investigations by Dender et al. (Dender 1996) on Copper benzoate also being a linear chain antiferromagnet. The Heisenberg model has a relation to the Hubbard model. According to Inui (Inui 1988) the pair hopping term of the Hubbard model can be mapped onto the next-to-nearest neighbour interaction of the antiferromagnetic Heisenberg (AFH) model. From the theoretical point of view, $1 - D$ spin chains are interesting because its critical properties are predicted by conformal symmetry under the hypothesis that this symmetry holds. Finally, $1 - D$ spin chains in the presence of magnetic fields and next-to nearest neighbour coupling display

* talk presented by H. Kröger

quite a rich phase structure. It is the purpose of this work to consider $1 - D$ spin chains and to present numerical results from exact diagonalization, discuss its finite-size analysis and critical behavior. We mainly consider static spin structure factors. In particular we analyze chains with next-to-nearest neighbour coupling allowing for frustration.

2 Heisenberg model and its extensions

Let us start by recalling the definition of various $1 - D$ spin models considered in the following: The classical model, describing next-neighbour interaction is given by the Ising model

$$H = J \sum_{i=1}^N S_i^z S_{i+1}^z, \quad (1)$$

where S_i^z is the z-component of spin i , taking the values $-1, +1$. The corresponding quantum model is the Heisenberg model,

$$H = J \sum_{i=1}^N \mathbf{S}_i \cdot \mathbf{S}_{i+1}, \quad (2)$$

where $\mathbf{S} = \boldsymbol{\sigma}/2$ and σ_a being the Pauli-matrices for the spin $1/2$ case. This is considered as the standard model of magnetism. In the case $J > 0$ the model describes antiferromagnetism, while $J < 0$ describes the ferromagnetic system. The following generalizations are of physical interest: The XXZ model describes the Heisenberg model with an anisotropy in z-direction,

$$H = J \sum_{i=1}^N S_i^x S_{i+1}^x + S_i^y S_{i+1}^y + \cos(\gamma) S_i^z S_{i+1}^z. \quad (3)$$

The Heisenberg model exposed to an external (classical) magnetic field is given by

$$H = J_1 \sum_{i=1}^N \mathbf{S}_i \cdot \mathbf{S}_{i+1} + J_B \sum_{i=1}^N \mathbf{B}_i \cdot \mathbf{S}_i. \quad (4)$$

If one takes into account next-to-nearest neighbour coupling of spins, the model becomes

$$H = J_1 \sum_{i=1}^N \mathbf{S}_i \cdot \mathbf{S}_{i+1} + J_2 \sum_{i=1}^N \mathbf{S}_i \cdot \mathbf{S}_{i+2}, \quad \alpha = J_2/J_1. \quad (5)$$

If the sign of J_1 and J_2 are such that one term favors parallel spins, while the other favors antiparallel spins, the system becomes frustrated. A model of particular interest with coupling beyond next neighbours is the Haldane-Shastry model (Haldane 1988), (Shastry 1988) (with periodic boundary conditions),

$$H = J \sum_{n=1}^{N-1} \sum_{m=1}^N \frac{1}{\sin^2(n\pi/N)} \mathbf{S}_m \cdot \mathbf{S}_{m+n}. \quad (6)$$

Below we will consider combinations of the above cases, e.g., the presence of a magnetic field and next-to-nearest neighbour coupling. In the following we will consider spin models with periodic boundary conditions.

2.1 Symmetries and integrability of Heisenberg model

The isotropic Heisenberg model has a number of symmetries and corresponding conserved quantities: There is translational symmetry. The translation operator $T = \exp[iP]$ defines the conserved quantum number of momentum P . There is also reflexion symmetry. The total spin $\mathbf{S} = \sum_{i=1}^N \mathbf{S}_i$ is conserved. There are more conserved quantities like, e.g., $F_3 = 2i \sum_{n=1}^N \epsilon_{ijk} S_{n-1}^i S_n^j S_{n+1}^k$ (Lüscher 1976), (Fabricius 1990). The existence of conserved quantities can be traced back to the existence of a set of commuting transfer matrices $T(\lambda)$, satisfying $[T(\lambda), T(\lambda')] = 0$ and $[T(\lambda), H] = 0$. The existence of such transfer matrices for the $1 - D$ Heisenberg model can be proved from inverse scattering theory or via the Yang-Baxter equations (Baxter 1980). The set of transfer matrices implies the existence of infinitely many conserved quantities like, e.g., the Hamiltonian $H \propto \frac{\partial}{\partial \lambda} \ln T(\lambda) \Big|_{\lambda=1/2} + \text{const.}$, the total spin squared $\mathbf{S}^2 \propto \frac{\partial^2}{\partial \lambda^2} T(\lambda) \Big|_{\lambda=\infty}$, or $F_3 \propto \frac{\partial^2}{\partial \lambda^2} \ln T(\lambda) \Big|_{\lambda=i/2} + \text{const.}$ (Fabricius 1990). Thus the Heisenberg model is an integrable system (Baxter 1980). Analytical solutions have been obtained via the Bethe ansatz (Bethe 1931). Using the Bethe ansatz, Hulthén (Hulthén 1938) has calculated the ground state energy per site in the thermodynamic limit $\epsilon_0 = 1/4 - \ln 2$ (corresponding to $J = 1/2$). Analytical information on the $1 - D$ model at the critical point can be obtained by making the assumption of conformal invariance. Cardy (Cardy 1986), (Cardy 1987) has shown that the spectrum of the transfer matrix is determined by conformal invariance. This predicts, e.g., the leading term of the finite size behavior of the ground state energy, or critical exponents of the spin-spin correlation function.

Recently, much analytic progress has been made in the Heisenberg and related spin models. Römer and Sutherland (Römer 1993) have computed the finite size dependence of the correlation function of the AFH model. The dynamical correlation function of the Calogero-Sutherland model has been computed by Ha (Ha 1994) and the single-particle Green's function of this model has been determined by Zirnbauer and Haldane (Zirnbauer 1995). Essler et al. (Essler 1996) have shown that correlation functions of the XXZ antiferromagnet near the critical magnetic field can be expressed in terms of solutions of Painlevé differential equations.

2.2 Quantum numbers of lowest state for finite chains

The quantum numbers of the lowest lying state for a finite spin chain have been analyzed by Fabricius et al. (Fabricius 1991). For a given total spin S and number of spins N one finds the quantum number of momentum P of the lowest lying

state to be as follows: For N even holds

$$P(\text{mod } 2\pi) = -\pi \times \begin{cases} S : N = 4, 8, 12, \dots \\ S + 1 : N = 2, 6, 10, \dots \end{cases} \quad (7)$$

For N odd, there is degeneration of momentum

$$\begin{aligned} P^+(\text{mod } 2\pi) &= -\pi \times \begin{cases} S(1 + 1/N) : N = 3, 7, 11, \dots \\ S(1 + 1/N) + 1 : N = 5, 9, 13, \dots \end{cases} \\ P^-(\text{mod } 2\pi) &= -\pi \times \begin{cases} S(1 - 1/N) + 1 : N = 3, 7, 11, \dots \\ S(1 - 1/N) : N = 5, 9, 13, \dots \end{cases} \end{aligned} \quad (8)$$

The absolute ground state corresponds to

$$\begin{aligned} P(S = 0) &= \begin{cases} 0 : N = 4, 8, 12, \dots \\ \pi : N = 2, 6, 10, \dots \end{cases} \\ P^\pm(S = 1/2) &= \mp\pi/2 \times \begin{cases} (1 + 1/N) : N = 3, 7, 11, \dots \\ (-1 + 1/N) : N = 5, 9, 13, \dots \end{cases} \end{aligned} \quad (9)$$

These are the quantum numbers corresponding to the isotropic Heisenberg model. In the case of next-to-nearest neighbour coupling the situation becomes more complicated. Then the quantum numbers of the lowest lying state will depend on the model parameters, like α .

2.3 Magnetization curve and susceptibility

Magnetization is defined by $\mathbf{M} = \langle \mathbf{S} \rangle / N$, it is a function of the external field \mathbf{B} . The functional dependence M versus B , the so-called magnetization curve is most easily obtained by computing the ground state energy ϵ per spin in a given spin sector and using

$$\frac{\partial \epsilon(M)}{\partial M} = B. \quad (10)$$

This follows from

$$\begin{aligned} H &= H|_{B=0} + \mathbf{B} \cdot \mathbf{S}, \\ E &= E|_{B=0} + \mathbf{B} \cdot \langle \mathbf{S} \rangle, \\ \epsilon &= E/N = \epsilon|_{B=0} + \mathbf{B} \cdot \mathbf{M}. \end{aligned} \quad (11)$$

The magnetization curve of the *AFH* with anisotropy at temperature zero is shown in Fig.[1]. One observes that when magnetization reaches its maximal value $M = 1/2$ (all spins aligned), then the magnetic field B becomes saturated. This can be understood as follows: For very long chains, i.e., near the thermodynamic limit, and close to saturation (nearly all spins aligned), then the change in energy when flipping a single spin becomes independent of the magnetization M . Thus $B = \partial \epsilon / \partial M = \text{const.}$ and B does not increase when M increases. The magnetization curve for the isotropic *AFH* model is analytically known to leading order in two limiting cases: (a) Weak magnetic field and (b) near saturation.

Fig. 1. Magnetization curve computed from Bethe ansatz equations for chain of length $N=2048$. γ is the anisotropy parameter. Taken from (Karch 1994a).

The case of weak magnetic field has been computed by Griffith (Griffith 1964) as well as by Yang and Yang (Yang 1966) using the Bethe ansatz and solving integral equations numerically. One obtains the expansion

$$M(B) = \frac{B}{\pi} \left[1 - a_1 \frac{1}{\ln B} - a_2 \frac{\ln |\ln B|}{\ln^2 B} - a_3 \frac{1}{\ln^2 B} + \dots \right]. \quad (12)$$

The lowest order is due to Griffith (Griffith 1964). The coefficient $a_1 = 1/2$ has been computed by Babujian (Babuian 1983) and $a_2 = 1/4$ has been obtained by Lee and Schlottmann (Lee 1987), while a_3 is unknown. The magnetization curve near saturation is known due to Yang and Yang (Yang 1966),

$$M(B) = \frac{1}{2} - \frac{\sqrt{2}}{\pi} \sqrt{B_c - B} + O(B_c - B), \quad (13)$$

and $B_c = 2$ for the isotropic case. From the magnetization curve, one obtains the magnetic susceptibility $\chi = \frac{\partial M(B)}{\partial B}$. The susceptibility corresponding to the magnetization curve of Fig.[1] is shown in Fig.[2]. Information on antiferromagnetic ordering is encoded in the ground state spin-spin correlation function $\langle 0 | \mathbf{S}(x) \cdot \mathbf{S}(0) | 0 \rangle$. For spin chains being isotropic with respect to coupling of x- and y-components of spin, one distinguishes the transverse and the longitudinal correlation function,

$$\omega_j(l, N) = 4 \langle 0 | S_{l+1}^j S_1^j | 0 \rangle, \quad j = 1, 2 : \text{transverse}, \quad j = 3 : \text{longitudinal}. \quad (14)$$

Luther and Peschel (Luther 1975) have found the following behavior of the correlation functions in the thermodynamic limit

$$\omega_j(l, N) \sim_{N \rightarrow \infty} \frac{(-1)^l}{l^{\eta_j}}. \quad (15)$$

Fig. 2. Susceptibility computed from Bethe ansatz equations for chain of length $N=2048$. γ is the anisotropy parameter. Taken from (Karbach 1994a).

For the isotropic Heisenberg model the critical exponents η_j obey $\eta_j = 1$ for $j = 1, 2, 3$. This follows from conformal symmetry (Luther 1975), (Bogoliubov 1986). Also based on conformal symmetry, Affleck et al. (Affleck 1989) have later predicted for the isotropic Heisenberg model a logarithmic correction to the long range behavior,

$$\langle S(x)S(0) \rangle \sim A \frac{(-1)^x}{x} (\ln x)^\sigma, \quad \sigma = 1/2. \quad (16)$$

3 Finite size scaling

Critical behavior of a physical theory can exist only in the thermodynamic limit ($N \rightarrow \infty$). Because very few models are soluble in the this limit, it is of great practical interest if physical information of the critical system can be obtained from a finite number of spins (finite volume). This has been answered by the theory of finite size scaling, introduced by Fisher (Fisher 1971). It can be summarized as follows: Suppose a model becomes critical at a temperature T_c . For the reduced temperature $t = (T - T_c)/T_c$ this corresponds to $t_c = 0$. Suppose there is an observable, which at the critical point behaves like a power law

$$\Gamma(t) \xrightarrow{t \rightarrow 0} \frac{1}{t^\phi}, \quad (17)$$

where ϕ is a critical exponent. In a finite volume N the observable is $\Gamma(t, N)$. The theory of finite-size scaling is based on the following assumption relating

Fig. 3. Transverse (a) and longitudinal (b) structure factor for $N = 4, \dots, 28$ and different anisotropy parameters γ . Taken from (Karbach 1994a).

the observable in the thermodynamic limit to the finite volume,

$$\Gamma(t, N) \xrightarrow{N \rightarrow \infty} \Gamma(t) f\left(\frac{N}{\xi(t)}\right), \quad (18)$$

where $\xi(t)$ is the correlation length in the thermodynamic limit and $f(z)$ is some function of a single variable. The correlation length has a critical behavior

$$\xi(t) \xrightarrow{t \rightarrow 0} \frac{1}{t^\nu}. \quad (19)$$

Fig. 4. Longitudinal structure factor versus scaling variable L_3 , Eq.(28), for $\gamma/\pi = 0, 0.1, 0.2, \dots, 0.5$ and $N = 4, 6, \dots, 28$.

The finite-size scaling hypothesis can be written in an equivalent form, originally proposed by Fisher (Fisher 1971),

$$\Gamma(t, N) \xrightarrow{N \rightarrow \infty} N^{\phi/\nu} g(Nt^\nu) \Big|_{t=\text{const.}} . \quad (20)$$

According to a theorem by Mermin and Wagner (Mermin 1966) the Heisenberg model in $D = 1$ and $D = 2$ dimensions does not have long range order and hence does not have a 2nd order phase transition for any finite temperature $T \neq 0$. The critical exponent ν of the correlation length has been computed in the thermodynamic limit for the XXZ spin model at the critical point $T_c = 0$ by Suzuki et al. (Suzuki 1992), using the Bethe ansatz. The result is $\nu = 1$.

4 Finite size analysis of spin-spin structure factors

Although the Bethe ansatz in principle allows for an exact calculation of the spin-spin correlation function, it is practically very difficult. As an alternative many workers have computed numerically correlation functions and structure factors. The following standard methods have been applied successfully to spin systems: exact diagonalization (Bonner 1964), coupled cluster - or $\exp(S)$ - method (Bishop 1995), quantum Monte Carlo method (Ceperley 1995), renormalization group techniques (White 1993), (Hallberg 1995). In the following we will focus on results obtained by exact diagonalization. Due to limitations in computing time and storage, exact diagonalization is possible only for small systems (for spin 1/2 chain of N spins in 1-D, the dimension of Hilbert space is 2^N). However, in the presence of a strong magnetic field B close to saturation nearly all spins

Fig. 5. Finite-size dependence of $\Delta_j(\gamma, p, N)$, Eq.(31), at momentum $p = \pi/2$.

are aligned. Setting up a Hilbert space basis by counting configurations of non-aligned (reversed) spins, the dimension will be much smaller. E.g., for $N = 50$ spins in the sector of magnetization $M = 2/5$, the dimension of Hilbert space is $d = 42376$. Thus spin chains of up to 56 spins have been diagonalized, using the Lanczos method and binary coding of spin configurations. The advantage of exact diagonalization is the high numerical precision allowing to carry out a finite size analysis and to extrapolate to the thermodynamic limit.

Fig. 6. Thermodynamic limit of transverse (T) and longitudinal (L) structure factor: $T1$, $L1$ finite-size analysis, $T2$, $L2$ conjecture of Ref. (Müller 1981), $T3$ exact result of XX -model. (a) $\gamma = \pi/2$, (b) $\gamma = 0$.

4.1 Structure factors in momentum space

Physical information on magnetic ordering is encoded in the spin-spin correlators. However, from the numerical point of view instead of analyzing the long range behavior of the correlation function it is easier to consider its Fourier transform, i.e., the spin structure factor in momentum space (Karbach 1993). The static spin structure factor is defined by

$$S_j(p, N) = \sum_{l=0}^{N-1} \omega_j(l, N) \exp[ipl], \quad p = 2\pi k/N, \quad k = 0, \dots, N-1. \quad (21)$$

One has the following correspondence

$$\begin{aligned} \text{x-space: } \langle S(x)S(0) \rangle &\sim \frac{(-1)^x}{x}, \\ \text{p-space: } \langle S(p) \rangle &\sim \sum_x e^{ipx} \frac{(-1)^x}{x} = \sum_x \frac{e^{i(p+\pi)x}}{x} \quad \text{divergent at } p = \pm\pi \end{aligned} \quad (22)$$

Thus the long distance behavior of the correlator manifests itself as divergence in p -space. Such behavior can be analyzed numerically for finite chains.

Fig. 7. Scaling function g_j in the finite-size scaling ansatz of Eq.(32) for $z = 2$.

4.2 Results for XXZ-model

For the XXZ -model with anisotropy angle γ , Eq.(3), the correlation function behaves as (Luther 1975)

$$\omega_j(\gamma, l) \sim c(\gamma) \frac{(-1)^l}{l \eta_j(\gamma)}, \quad \eta_1(\gamma) = \eta_3^{-1}(\gamma) = 1 - \gamma/\pi, \quad 0 \leq \gamma \leq \pi/2. \quad (23)$$

Note that $\eta_1(\gamma) \cdot \eta_3(\gamma) = 1$. The corresponding structure factor behaves as

$$S_j(\gamma, p) \sim a_j + b_j [1 - p/\pi]^{\eta_j - 1}. \quad (24)$$

Because $\eta_1(\gamma) < 1$ and $\eta_3(\gamma) > 1$, at momentum $p = \pi$ the transverse structure factor becomes divergent, while the longitudinal structure factor remains finite. This behavior changes when $\gamma \rightarrow 0$ (isotropic limit). For finite systems the corresponding correlation function and structure factor is given by

$$\begin{aligned} \omega_j(\gamma, l) &\sim \tilde{c}_j(\gamma) \frac{(-1)^l}{l^{\eta_j(\gamma)}} \exp[l/\xi_j(\gamma, N)], \\ S_j(\gamma, p) &\sim \tilde{a}_j + \tilde{b}_j [(1 - p/\pi)^2 + 1/\xi_j^2(\gamma, N)]^{\eta_j - 1}, \end{aligned} \quad (25)$$

where $\xi_j(\gamma, N)$ is the correlation length in the finite system. The correlation length has the following critical behavior when $\cosh(\gamma') > 1$ and $\gamma' \rightarrow 0$ (Johnson 1973)

$$\xi \longrightarrow \frac{1}{8} \exp \left[\frac{\pi^2}{2\gamma'} \right] \quad \text{divergent at } \gamma' = 0. \quad (26)$$

The structure factor diverges at $p = \pi$ when $\gamma' \rightarrow 0$ (Singh 1989)

$$S_j(\gamma', p = \pi, N = \infty) \longrightarrow_{\gamma' \rightarrow 0} \frac{1}{\gamma'^{\lambda_j}}, \quad \lambda_1 = 3/2, \lambda_3 = 2. \quad (27)$$

The longitudinal and transverse structure factors for finite systems are shown in Fig.[3]

Fig. 8. Scaling behavior of transverse structure factor at $p = \pi$, compared with finite-size scaling ansatz of Eq.(33).

Now let us look at the scaling properties of the structure factors. One can ask the following questions: (a) Does a scaling variable L_j exist such that $S_j(\gamma, p, N) =$

$S_j(\gamma, L_j(\gamma, p, N))$? (b) How does $S_j(\gamma = 0, p, N = \infty)$ behave when $p \rightarrow \pi$? (c) What is the leading finite-size behavior of $S_j(\gamma, p, N)$ when $p < \pi$? (d) How does $S_j(\gamma, p = \pi, N)$ behave when N is large and $\gamma \rightarrow 0$? Karbach and Mütter (Karbach 1993) have suggested to use $L_3(\gamma, p)$ as scaling variable, given by

$$L_3(\gamma, p) = \frac{\eta_3(\gamma)}{\eta_3(\gamma) - 1} \left[1 - (1 - p/\pi)^{\eta_3(\gamma) - 1} \right], \quad p < \pi. \quad (28)$$

Haldane and Shastry (Haldane 1988), (Shastry 1988) have shown that

$$\lim_{\gamma \rightarrow 0} L_3(\gamma, p) = -\ln(1 - p/\pi), \quad p < \pi \quad (29)$$

is the exact structure factor of the Haldane-Shastry model, Eq.(6), with periodic boundary conditions. Numerical studies (Karbach 1993), (Karbach 1994b) show the following scaling behavior. Fig.[4] gives a plot of the longitudinal structure factor versus the scaling variable L_3 . The data points lie close to a line of slope one when $p < \pi$. Similar but less impressive scaling holds for the transverse component. Scaling deviations can be further analyzed by looking at

$$\Delta_j(\gamma, p, N) = S_j(\gamma, p, N) - L_j(\gamma, p). \quad (30)$$

It is remarkable that at $\gamma = \pi/2$ (XX -model) no finite-size dependence exists,

Fig. 9. Longitudinal structure factor versus momentum p and magnetization M for $N = 20, 22, \dots, 28$. The ridge occurs at softmode $p_3(M)$, Eq.(34).

$S_3(\gamma = \pi/2, p, N) = 2p/\pi$. For $p < \pi$ one makes the following finite size ansatz

$$\Delta_j(\gamma, p, N) = \Delta_j(\gamma, p, N = \infty) + \frac{c_j(\gamma, p)}{N^2}, \quad p < \pi. \quad (31)$$

The finite size behavior is shown in Fig.[5] and confirms the leading $1/N^2$ behavior when approaching the thermodynamic limit. The case $\gamma = \pi/2$ corresponds to the XX -model which is exactly soluble. Fig.[6] shows the thermodynamic limit of the structure factors. For $\gamma = \pi/2$ comparison with the exact result

Fig. 10. Transverse structure factor at $M = 1/4$. (a) Finite-size behavior at $p = \pi$, Eq.(35). (b) Momentum dependence for $p \rightarrow \pi$, Eq.(36).

shows agreement. The above analysis is not valid when approaching $p = \pi$. The following finite-size scaling ansatz can be made in the combined limit $N \rightarrow \infty$, $p \rightarrow \pi$,

$$S_j(\gamma, p, N) \xrightarrow{p \rightarrow \pi, N \rightarrow \infty} S_j(\gamma, p, N = \infty) g_j(\gamma, z)|_{z=(1-p/\pi)N=\text{const.}} \quad (32)$$

The scaling function g_j is shown in Fig.[7]. The transverse structure factor is singular at $p = \pi$. At the singularity the following finite-size ansatz can be made

$$S_1(\gamma, p = \pi, N) \xrightarrow{N \rightarrow \infty} r_1 \frac{\eta_1}{\eta_1 - 1} [1 - \sin(\eta_1 \pi/2)(a_1/N)^{\eta_1 - 1}]. \quad (33)$$

Numerical data compared with this ansatz are shown in Fig.[8].

5 AFH model with next-to-nearest neighbour coupling and external magnetic field

Antiferromagnetic order is manifested in the Heisenberg model via singularities of structure factors when $p \rightarrow \pi$, $N \rightarrow \infty$ and $z = (1 - p/\pi)N = \text{const}$. Then

the transverse structure factor becomes infinite, while the longitudinal structure factor remains finite. This antiferromagnetic order can be destructed (a) by switching on an external uniform magnetic field B or (b) by frustration (i.e., nearest neighbour and next-to-nearest neighbour coupling do not favour the same alignment pattern). Such will be examined in this section. As a result it turns out that there are similarities between the anisotropic chain (XXZ) and the chain with next-to-nearest neighbour coupling.

Fig. 11. Longitudinal structure factor at $M = 1/4$. (a) Finite-size behavior at softmode $p_3(M)$, Eq.(38). (b) Momentum dependence for $p \rightarrow p_3(M)$, Eq.(39).

5.1 Presence of external magnetic field

When considering the Heisenberg Hamiltonian in the presence of a uniform external magnetic field \mathbf{B} , Eq.(4), (with $\mathbf{B}_i = \mathbf{B} = B\mathbf{e}_z$ and $J_B = 1$), one observes in the spectrum of the Hamiltonian the following property: Zero-frequency modes $\omega(p_{soft}) = 0$ emerge at non-zero "soft-mode" momenta p_{soft} . These modes show up in the dynamical structure factors $S_1(\omega, p)$ and $S_3(\omega, p)$ (Fledderjohann 1996). The momenta depend on the field B , or the magnetization M , respectively. One has

$$p_1(M) = 2\pi M, \quad p_3(M) = \pi(1 - 2M). \quad (34)$$

The critical exponents η_j are supposed to govern the long distance behavior of the static structure factors and the infra-red behavior of the dynamical struc-

ture factors. Now $\eta_i = \eta_i(M)$ become field dependent. Provided that the low-lying excitation spectrum is governed by conformal symmetry, one can make analytical predictions. Numerical studies (Karbach 1995), (Fledderjohann 1996) show the following behavior. In Fig.[9] the longitudinal structure factor is plotted versus momentum and magnetization. The results correspond to chains of $N = 20, 22, \dots, 28$ spins. The structure factor is a smooth function except for a ridge at the soft-mode. One observes that the soft-mode moves with magnetization. On the other hand, the transverse structure factor diverges at $p = \pi$ when $N \rightarrow \infty$ like

$$S_1(p = \pi, M, N) \xrightarrow{N \rightarrow \infty} N^{1-\eta_1(M)}. \quad (35)$$

For $M = 1/4$ one finds, e.g., $\eta_1 = 0.65$, shown in Fig.[10a]. The exponent η_1 governs also the approach to the singularity at $p = \pi$,

$$S_1(p, M, N = \infty) \xrightarrow{p \rightarrow \pi} (1 - p/\pi)^{\eta_1(M)-1}, \quad (36)$$

which is shown in Fig[10b]. When approaching the soft-mode momentum $p_1(M)$, one finds the behavior

$$S_1(p, M, N = \infty) \xrightarrow{p \rightarrow p_1(M) \pm 0} (1 - p/p_1(M))^{\eta_1^\pm(M)-1}. \quad (37)$$

Numerical results indicate that $\eta_1^-(M)$ and $\eta_1^+(M)$ do not necessarily agree. The corresponding behavior of the longitudinal structure factor is as follows. The finite size behavior at the soft-mode momentum $p_3(M)$ is given by

$$S_3(p_3(M), M, N) \xrightarrow{N \rightarrow \infty} N^{1-\eta_3(M)}. \quad (38)$$

This is displayed in Fig.[11a]. Approaching the soft-mode from the left one has

Fig. 12. Magnetization curve for $\alpha = 0$ and $\alpha = 1/4$. The solid line is the Bethe ansatz solution with $N=2048$ spins.

$$S_3(p, M, N = \infty) \xrightarrow{p \rightarrow p_3(M) - 0} (1 - p/p_3(M))^{\eta_3^-(M) - 1}, \quad (39)$$

shown in Fig.[11b]. There is indication for $\eta_3(M) = \eta_3^-(M)$. However, if $\eta_3^+(M)$ and $\eta_3^-(M)$ agree is an open question.

5.2 Next-to-nearest neighbour coupling

Now let us consider the model Hamiltonian including next-to-nearest neighbour coupling and the presence of a magnetic field, given by a combination of Eqs.(5, 4). This model has a rich phase structure, depending on the parameters J_1 , J_2 and B . There is a ferromagnetic phase, an antiferromagnetic phase and a frustrated phase (Farnell 1994). Haldane (Haldane 1982) has shown that within the antiferromagnetic phase there is a phase transition at α_c between a spin-fluid phase ($\alpha < \alpha_c$) and a dimer phase ($\alpha > \alpha_c$). The transition point has been determined to be $\alpha_c = 0.24$ (Okamoto 1992). Related to this is Gluzman's (Gluzman 1994) prediction of the occurrence of a plateau in the magnetization curve. Moreover, it is remarkable that the model is exactly soluble at $\alpha = 1/2$, $B = 0$, called Majumdar-Ghosh point (Majumdar 1969). One can ask: Where are the observable differences in the model with and without next-to-nearest neighbour coupling, i.e., $\alpha \neq 0$ and $\alpha = 0$? Numerical studies by Schmidt et al. (Schmidt 1996) and Gerhardt et al. (Gerhardt 1996) give the following information. Firstly, one observes in the magnetization curve near saturation the following characteristic behavior,

$$M(\alpha = 1/4, B) \xrightarrow{B \rightarrow B_s} 1/2 - \text{const.} \times (B_s - B)^{1/4}, \quad (40)$$

in contrast to the square root behavior for $\alpha = 0$, given by Eq.(13). This is shown in Fig.[12]. In the presence of an external magnetic field and next-to-nearest neighbour coupling, the structure factors develop singularities at soft-mode momenta, given by Eq.(34). Now the strength of the singularity will depend on the the frustration parameter α . The transverse structure factor and the longitudinal structure factor for fixed values of α but different values of magnetization M are shown in Fig.[13a] and [13b], respectively. Fig.[14] displays the structure factors for fixed M but different values of α . The critical exponents η_i will now depend on M and α . The finite-size dependence of the transverse structure factor at $p = \pi$ is described by

$$S_1(\alpha, p = \pi, M, N) \xrightarrow{N \rightarrow \infty} A_1(\alpha, M) + B_1(\alpha, M)N^{1-\eta_1(\alpha, M)}. \quad (41)$$

E.g., one finds $\eta_1(\alpha = 0, M = 1/4) = 0.65$, while $\eta_1(\alpha = 1/4, M = 1/4) = 1.16$. Similarly, the longitudinal structure factor at the soft-mode $p_3(M)$ behaves as

$$S_3(\alpha, p = p_3(M), M, N) \xrightarrow{N \rightarrow \infty} A_3(\alpha, M) + B_3(\alpha, M)N^{1-\eta_3(\alpha, M)}. \quad (42)$$

E.g., one finds $\eta_3(\alpha = 0, M = 1/4) = 1.5$, while $\eta_3(\alpha = 1/4, M = 1/4) = 0.84$. Those critical exponents extracted from Eqs.(41, 42) are given in Tab.[1] as a function of α . Based on the assumption that conformal symmetry holds, one

Fig. 13. Transverse structure factor (a) and longitudinal structure factor (b) versus momentum p for fixed magnetization $M = 1/4$ but different values of α .

would expect $\eta_1 \cdot \eta_3 = 1$. The numerical data for most values of α deviate from the expected result by a few percent. However, special attention should be paid to the region $\alpha \sim -0.2$ and the region $\alpha \geq 0.4$. For $\alpha = -0.2$ Eq.(42) does not yield a value of η_3 . It turns out that the finite-size dependence is very weak in this region ($B_3(\alpha, M)$ is very small) and may even vanish for some value of α . Secondly, for $\alpha \geq 0.4$, $\eta_1 \cdot \eta_3$ deviates substantially from the value one. The reason is most likely the following: The structure factors have been computed in the sector corresponding to quantum numbers of the Heisenberg model, Eq.(9). For $\alpha \geq 0.4$, those are presumably no longer the quantum numbers of the ground state, hence the critical exponents η_i do not correspond to the ground state but to some excited state.

Fig. 14. Transverse structure factor (a) and longitudinal structure factor (b) versus momentum p for fixed $\alpha = 1/4$ but different values of M .

Table 1. Critical exponents η_i for $M = 1/4$ versus α

α	-0.5	-0.4	-0.3	-0.2	-0.1	0	0.1	0.2	0.25	0.3	0.4	0.5
η_1	0.39	0.42	0.45	0.50	0.56	0.65	0.78	1.00	1.16	1.36	2.74	3.53
η_3	2.52	2.45	2.34	?	1.66	1.49	1.26	0.98	0.84	0.70	0.47	0.32
$\eta_1 \cdot \eta_3$	0.98	1.03	1.06	?	0.93	0.97	0.98	0.98	0.97	0.94	1.28	1.13

6 Summary and outlook

The 1-D spin 1/2 AFH model in the presence of an external magnetic field and with next-to-nearest neighbour coupling can be solved "exactly" by diagonalization (via Lanczos) of chains of up to 50 spins (depending on M). For the ground state properties of the model this yields data with high numerical precision allowing for finite-size scaling analysis and extraction of critical exponents. Here we have concentrated on static spin structure factors. One finds a different behavior for $\alpha < \alpha_c$ and $\alpha > \alpha_c$. The difference is observed in the strength of the singularities of structure factors and in the magnetization curve near saturation. Much interesting physics is to be explored when going into D=2,3 dimensions (e.g., prediction of plateaus in the magnetization curve). Exact diagonalization is presently limited in D=2 to 7×7 spins (with helical boundary conditions). To analyze critical behavior in D=2, new methods yielding numerically precise results for a larger number of spins are needed.

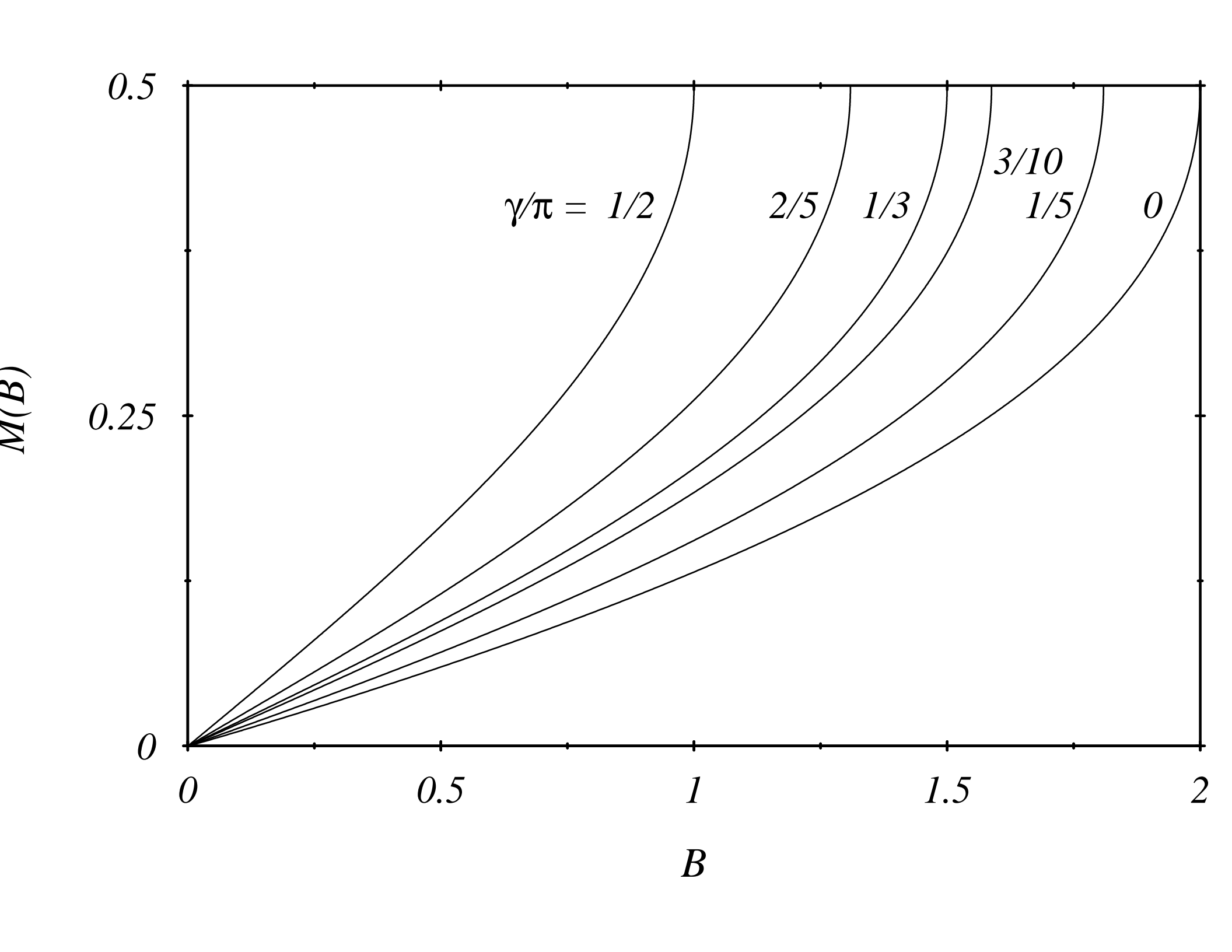
Acknowledgement

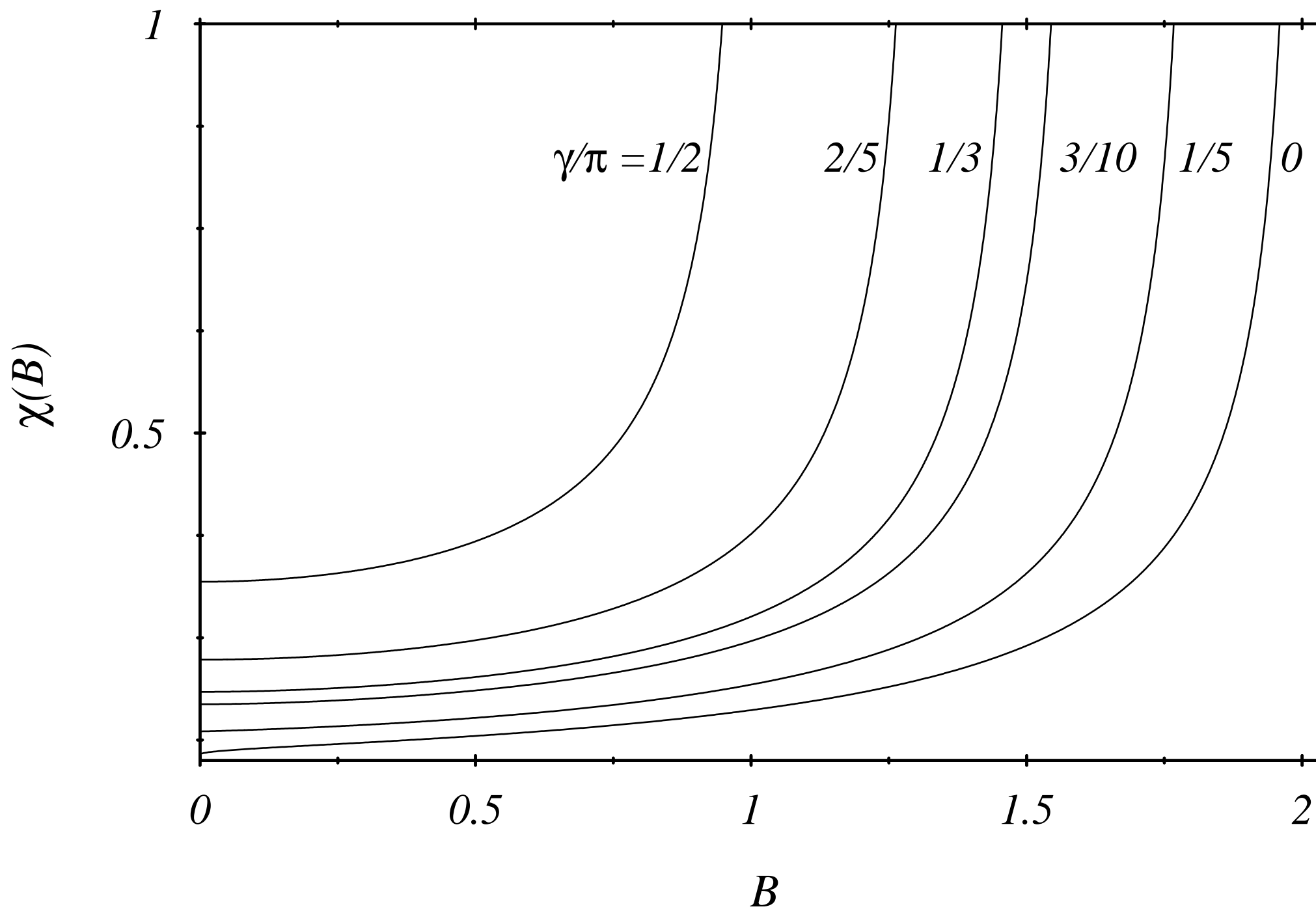
One of the authors (H.K.) is grateful for support by NSERC Canada.

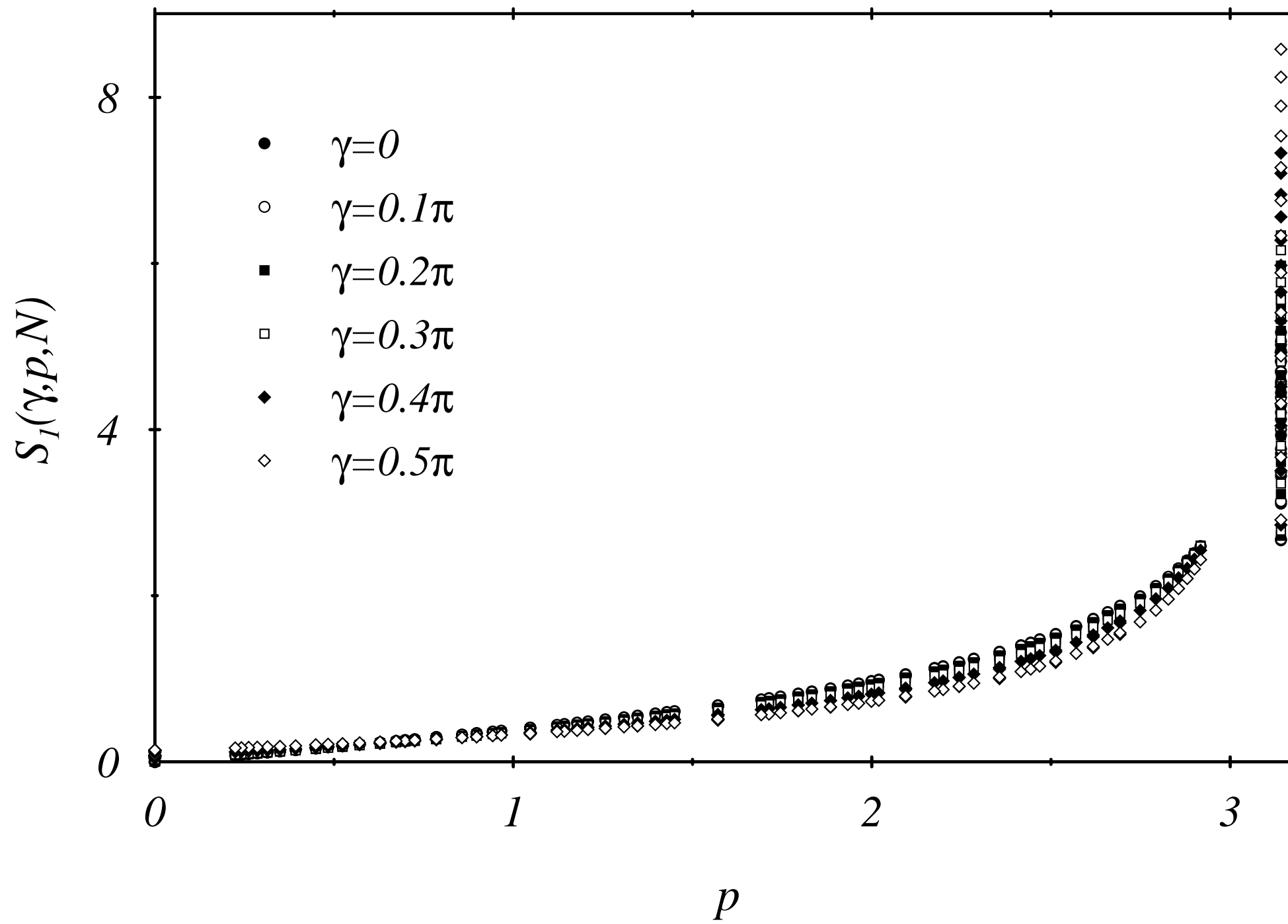
References

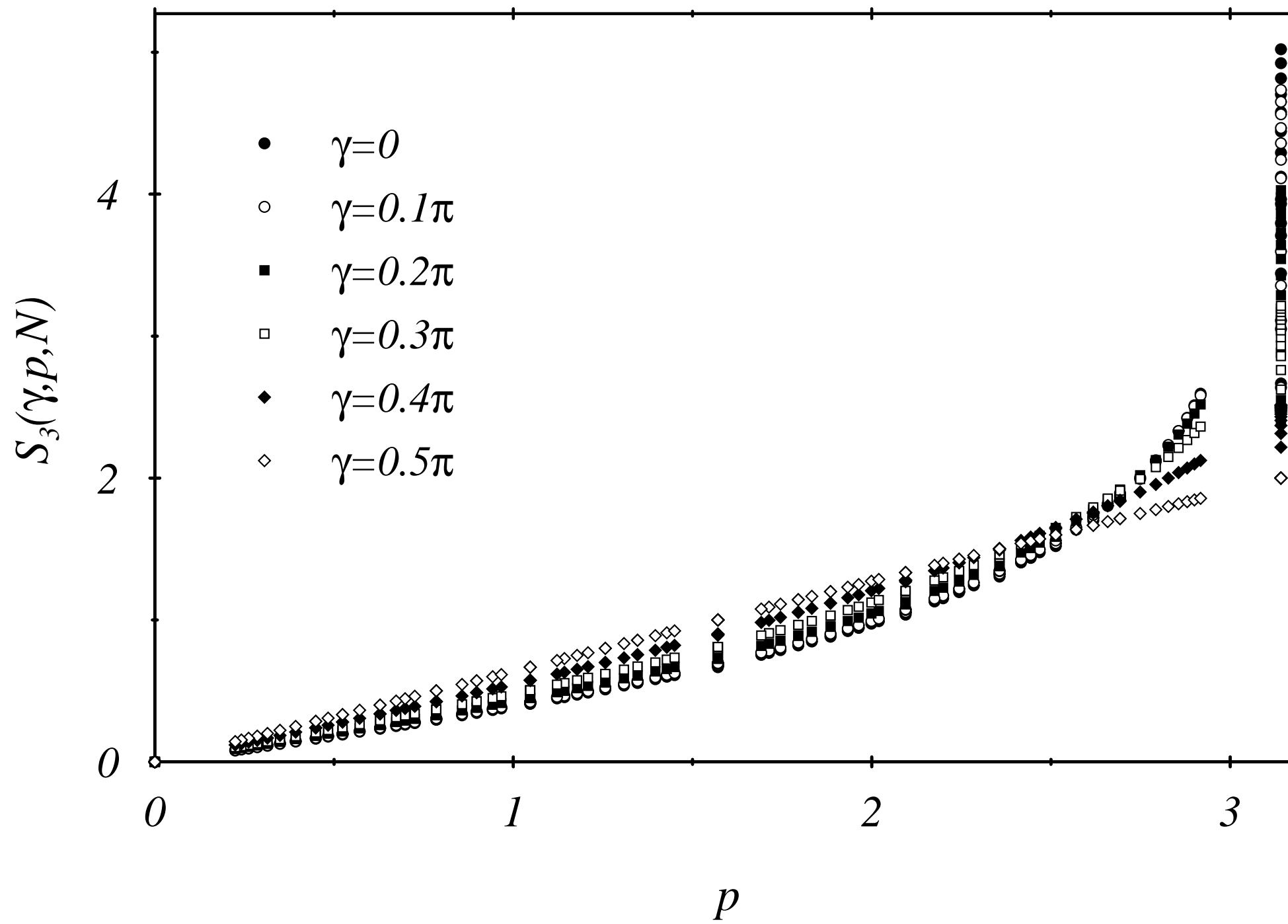
- I. Affleck, D. Gepner, H. Schulz and T. Ziman, *J. Phys.* A22(1989)511.
 H.M. Babujian, *Nucl. Phys.* B215(1983)317.
 R.J. Baxter, *Exactly Solved Models in Statistical Mechanics*, Academic Press (1980).
 J. Bernasconi, T. Schneider, *Physics in One Dimension*, Springer, New York (1981).
 H.A. Bethe, *Z. Phys.* 71(1931)205.
 R.F. Bishop, in *Recent Progress in Many-Body Theories*, eds. E. Schachinger et al., Plenum, New York (1995), p.195;
 see also R.F. Bishop, talk at this Workshop.
 N.M. Bogoliubov, A.G. Izergin and V.E. Korepin, *Nucl. Phys.* B275(1986)687.
 J.C. Bonner and M.E. Fisher, *Phys. Rev.* 135(1964)17640.
 J.L. Cardy, *Nucl. Phys.* B270(1986)186.
 J.L. Cardy, in *Phase Transitions and Critical Phenomena*, Ed. C. Domb and J.L. Lebowitz, Academic Press (1987), Vol.11.
 J.L. Cardy, ed., *Finite-Size Scaling*, North Holland, Amsterdam (1988).
 D.M. Ceperley, in *Recent Progress in Many-Body Theories*, eds. E. Schachinger et al., Plenum, New York (1995), p.455.
 D.C. Dender, D. Davidović, D.H. Reich, C. Broholm, K. Lefmann and G. Aeppli, *Phys. Rev.* B53(1996)2583.
 J.D. Dunitz, *Acta Cris.* 10(1957)307.
 F.H.L.Essler, H. Frahm, A.R. Its and V.E. Korepin, *solv-int*/9604005.
 K. Fabricius, K.H. Mütter and H. Grosse, *Phys. Rev.* B42(1990)4656.
 K. Fabricius, U. Löw, K.H. Mütter and P. Ueberholz, *Phys. Rev.* B44(1991)7476.
 D.J.J. Farnell and J.B. Parkinson, *J. Phys. Condens. Matter* 6(1994)5521.
 M.E. Fisher, in *Critical Phenomena*, *Proceed. 51st Enrico Fermi Summer School*, ed. M.S. Green, Academic Press, London (1971).

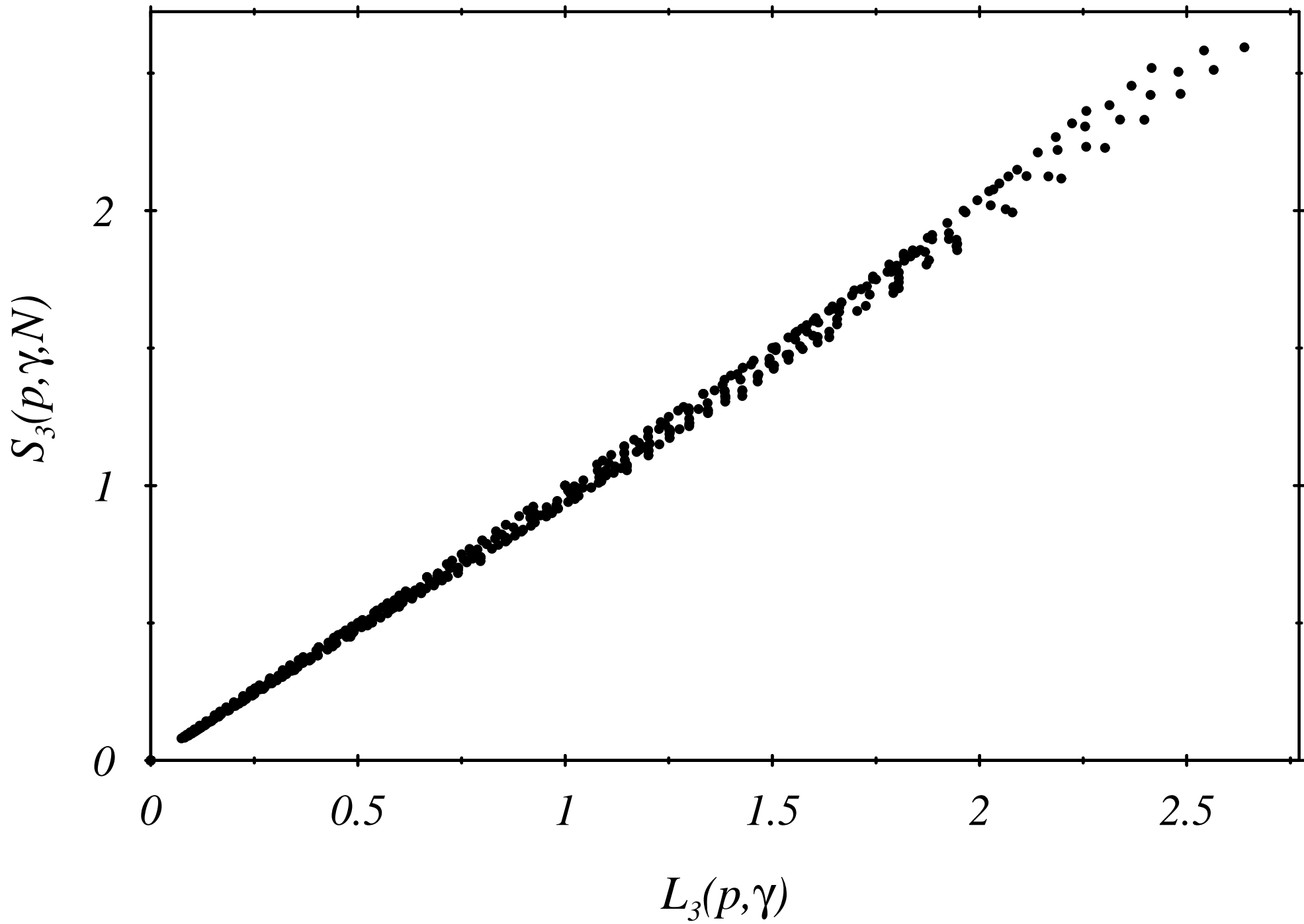
- M.N. Fisher and M.N. Barber, Phys. Rev. Lett. 28(1972)1516.
A. Fledderjohann, C. Gerhardt, K.H. Mütter, A. Schmitt and M. Karbach, Phys. Rev. B54(1996)7168.
C. Gerhardt, A. Fledderjohann, E. Aysal, K.H. Mütter, J.F. Audet and H. Kröger, J. Phys. Condens. Matter, subm.
T. Giamarchi and H.J. Schulz, Phys. Rev. B39(1989)4620.
S. Gluzman, Phys. Rev. B49(1994)11962.
R.B. Griffith, Phys. Rev. A133(1964)768.
Z.N.C. Ha, Phys. Rev. Lett. 73(1994)1574.
F.D.M. Haldane, Phys. Rev. B25(1982)4928; B26(1982)5257.
F.D.M. Haldane, Phys. Rev. Lett. 60(1988)635.
K.A. Hallberg, P. Horsch and G. Martinez, Phys. Rev. B52(1995)R719.
K. Hallberg, X.Q.G. Wang, P. Horsch and A. Moreo, Phys. Rev. Lett. 76(1996)4955.
L. Hulthén, Ark. Mat. Astr. Fys. 26(1938)1.
M. Inui, S. Doniach and M. Gabay, Phys. Rev. B38(1988)6631.
J.D. Johnson, S. Krinsky and B.M. McCoy, Phys. Rev. A8(1973)2526.
M. Karbach and K.H. Mütter, Z. Phys. B90(1993)83.
M. Karbach, Ph.D. Thesis, Universität Wuppertal (1994a).
M. Karbach, K.H. Mütter and M. Schmidt, Phys. Rev. B50(1994b)9281.
M. Karbach, K.H. Mütter and M. Schmidt, J. Phys. Condens. Matter. 7(1995)2829.
K.J.B. Lee and P. Schlottmann, Phys. Rev. B36(1987)466.
M. Lüscher, Nucl. Phys. B117(1976)475.
A. Luther and I. Peschel, Phys. Rev. B12(1975)3908.
C.K. Majumdar and D.K. Ghosh, J. Math. Phys. 10(1969)1388; 1399.
F. Mazzi, Acta Cryst. 8(1955)137.
N.D. Mermin and H. Wagner, Phys. Rev. Lett. 17(1966)1133.
G. Müller, H. Thomas and J.C. Bonner, Phys. Rev. B24(1981)1429; J. Phys. C14(1981)3399.
K. Okamoto and K.Nomura, Phys. Lett. A169(1992)433.
R.A.Römer and B. Sutherland, Phys. Rev. B48(1993)6058.
M. Schmidt, C. Gerhardt, K.H. Mütter and M. Karbach, J. Phys. Condens. Matter 8(1996)553.
B.S. Shastry, Phys. Rev. Lett. 60(1988)639.
R.R.P. Singh, M.E. Fisher and R. Shankar, Phys. Rev. B39(1989)2562.
J. Suzuki, T. Nagao and M. Wadati, Int. J. Mod. Phys. B6(1992)1119.
D.A. Tennant, R.A. Cowley, S.E. Nagler and A. Tsvelik, Phys. Rev. B52(1995)13368.
S.R. White, Phys. Rev. B48(1993)10345.
C.N. Yang and C.P. Yang, Phys. Rev. 150(1966)321; *ibid* 150(1966)327; *ibid* 151(1966)258.
M.R.Zirnbauer and F.D.M. Haldane, cond-mat/9504108.

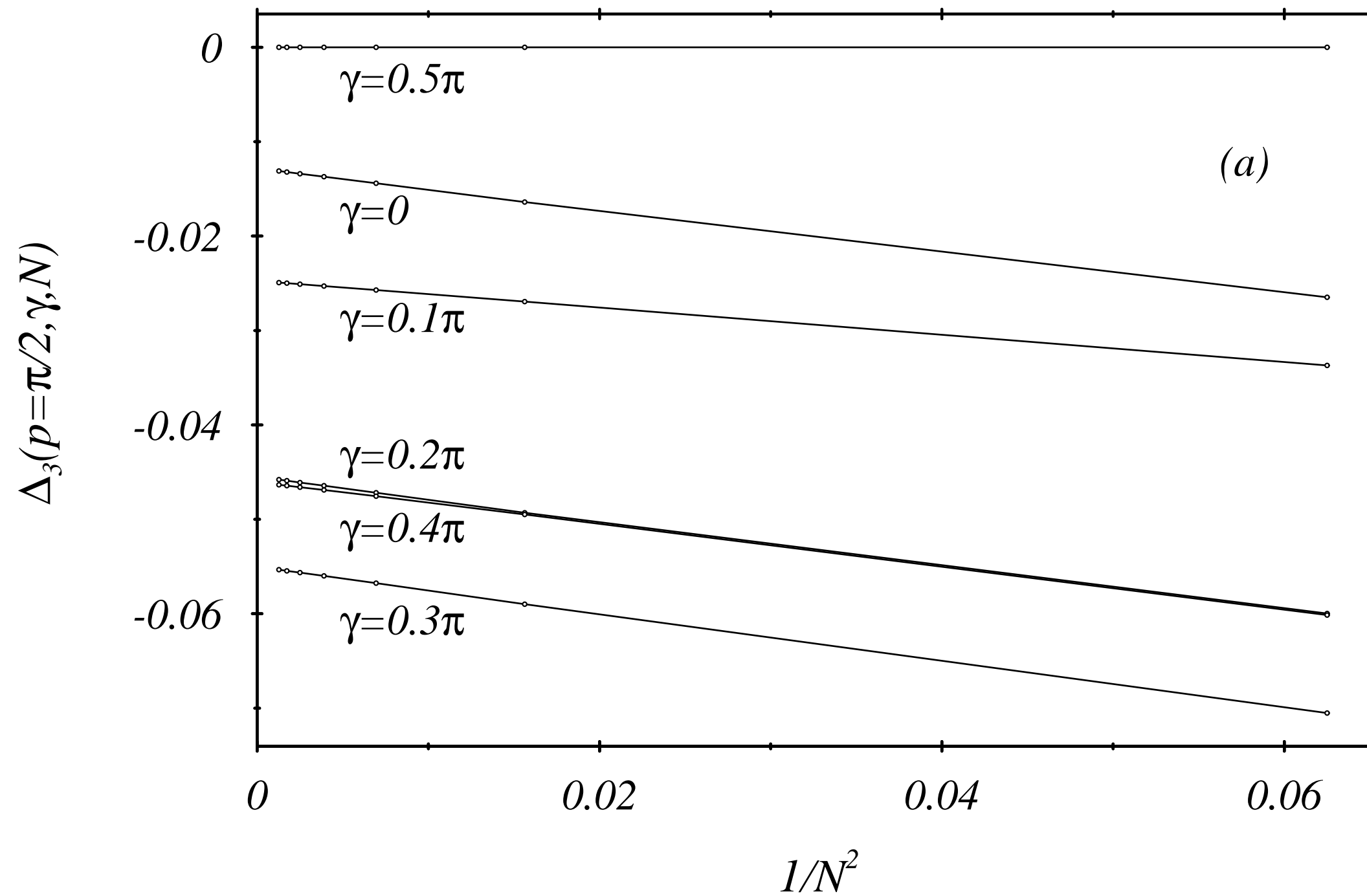


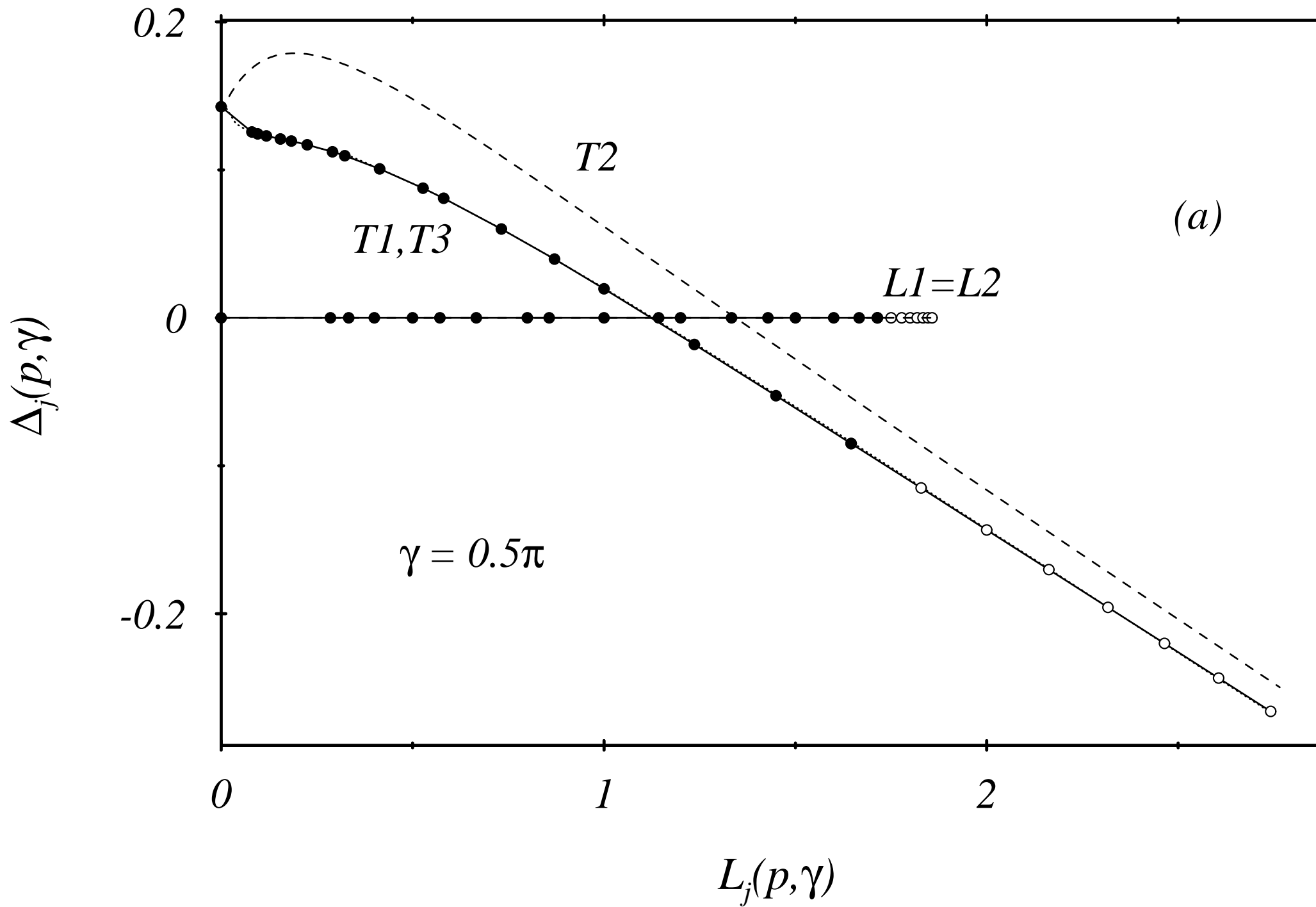


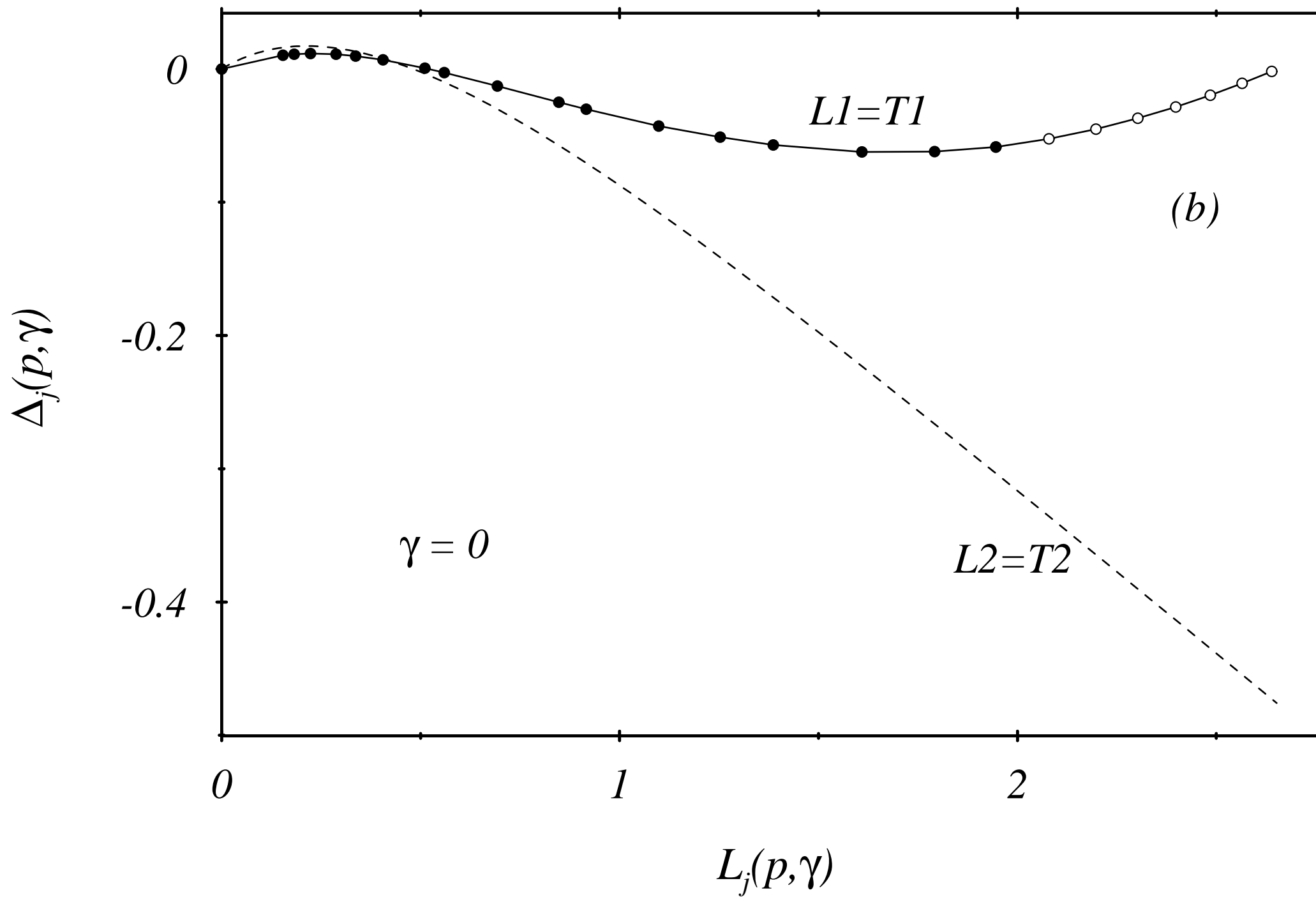


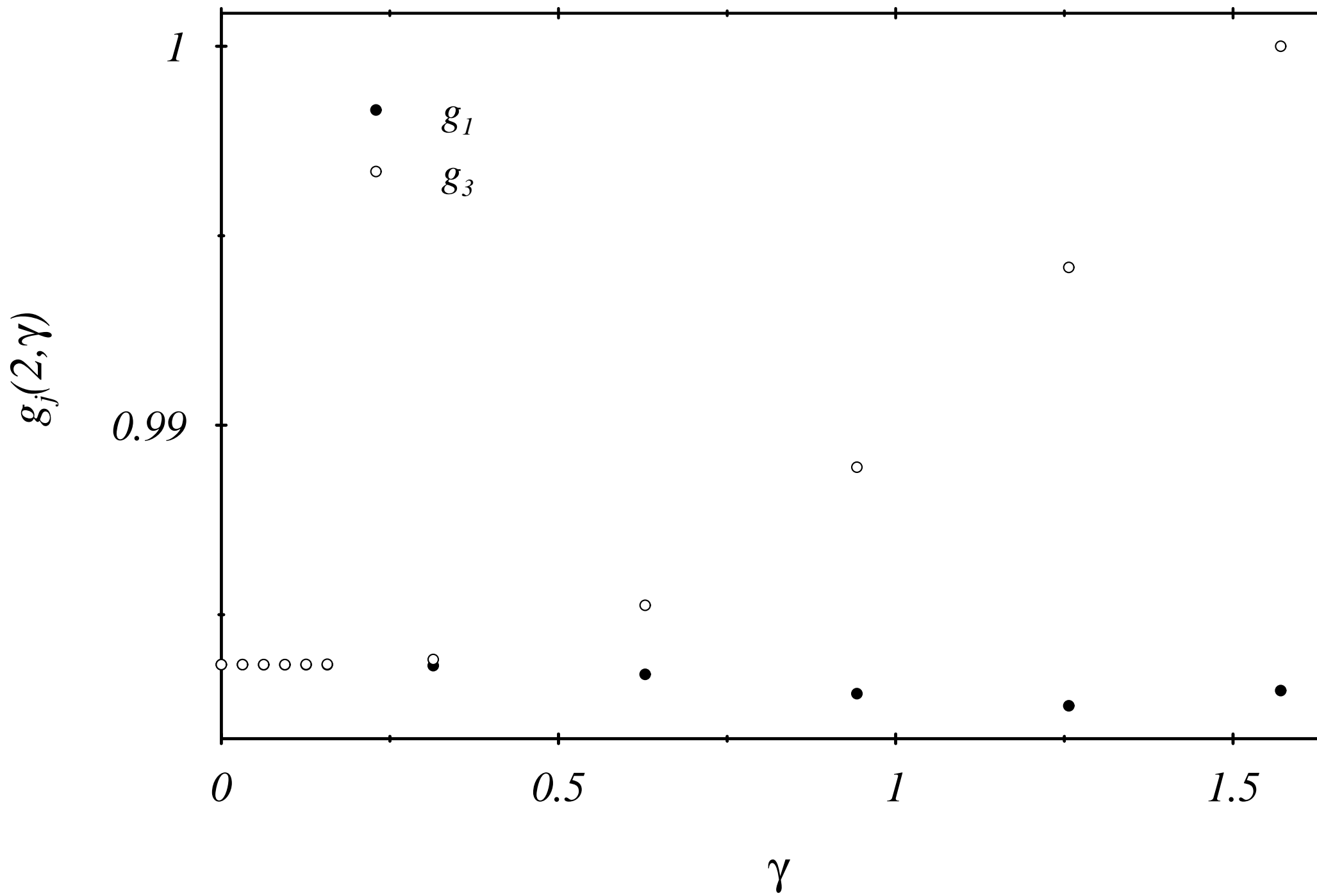


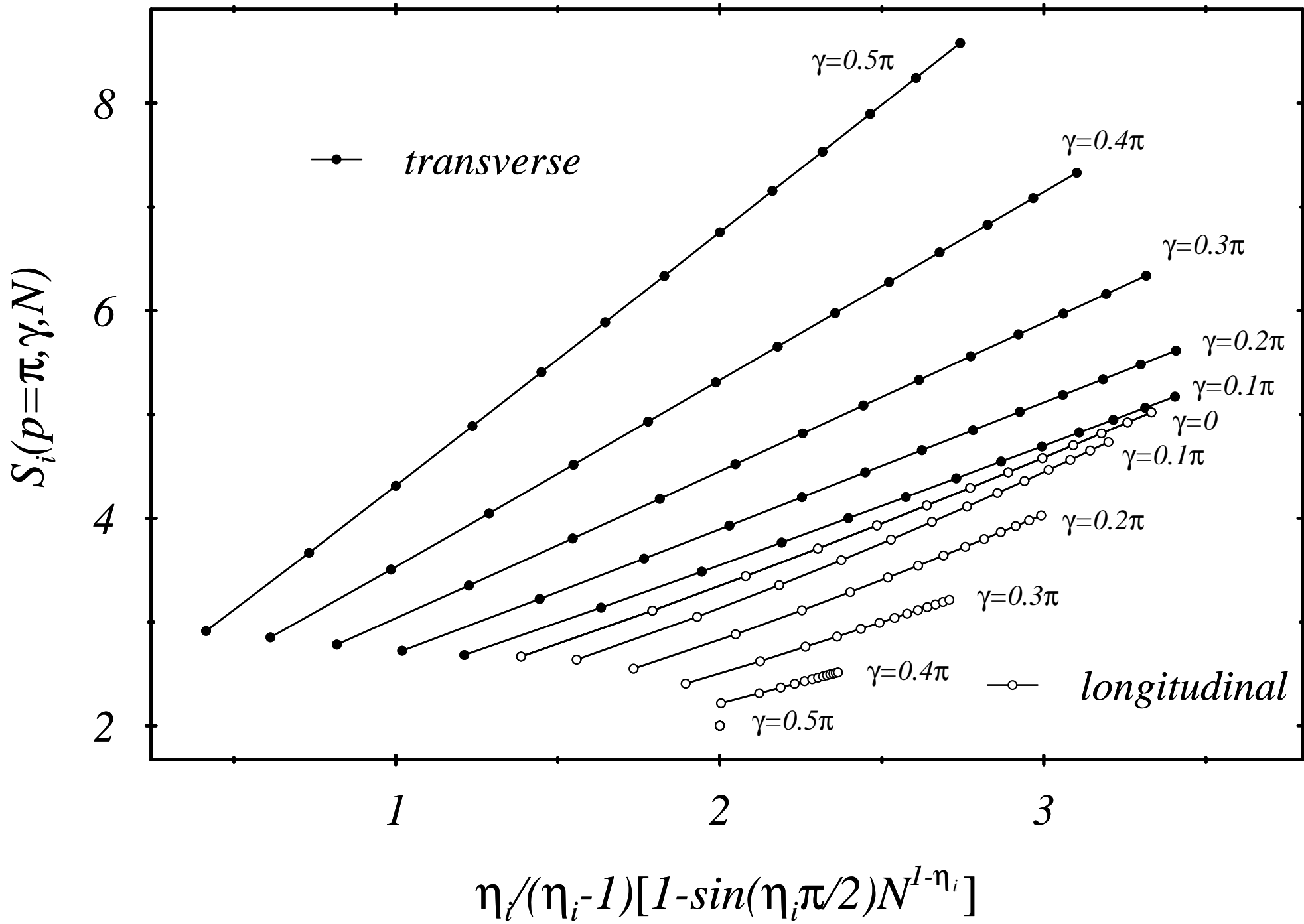


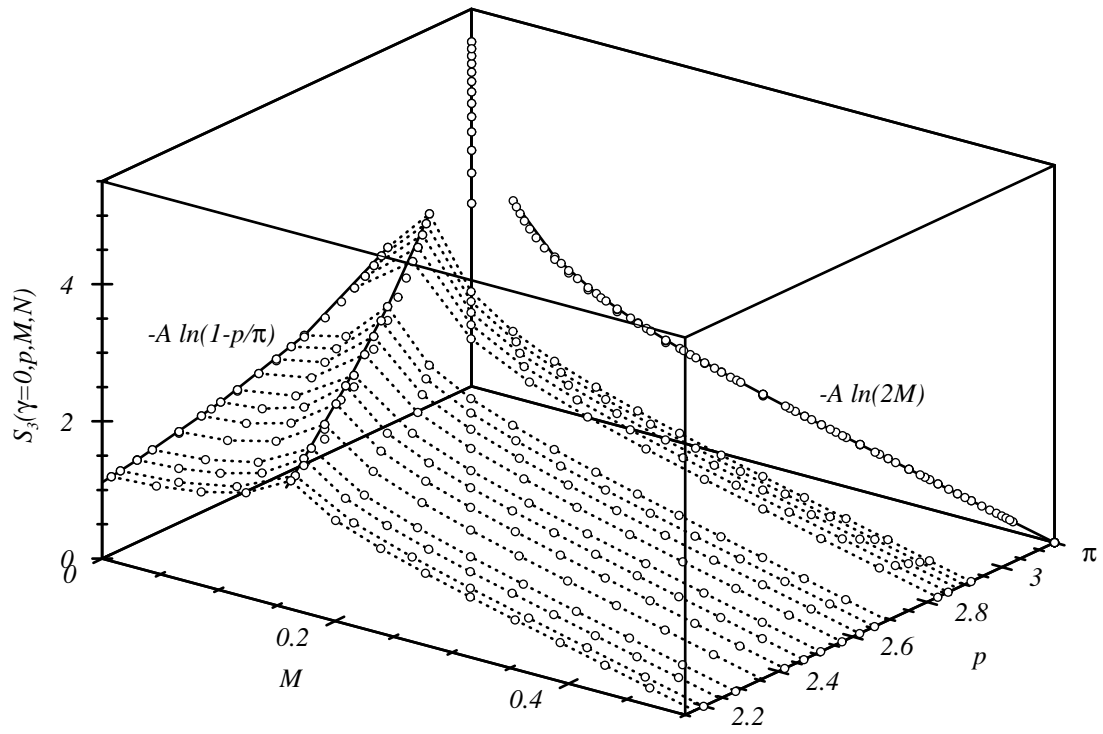












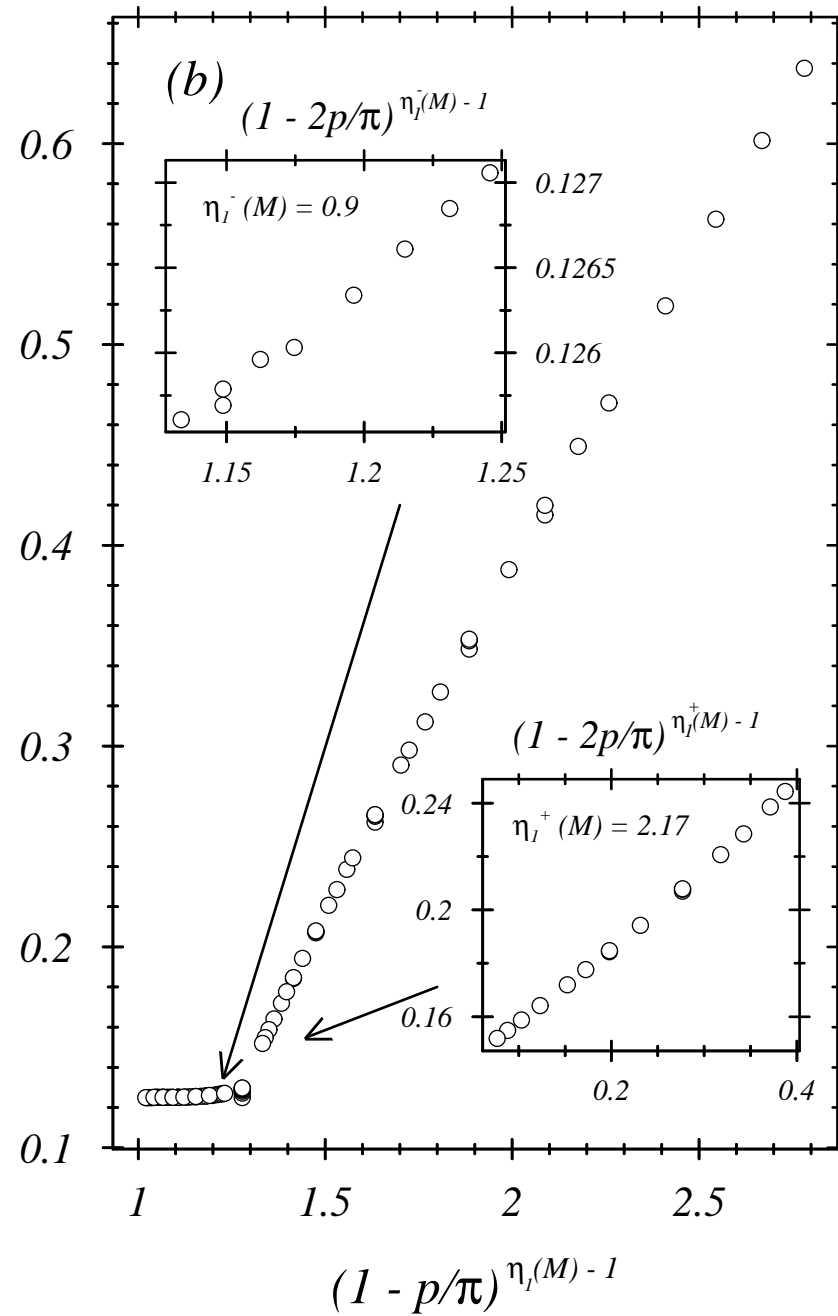
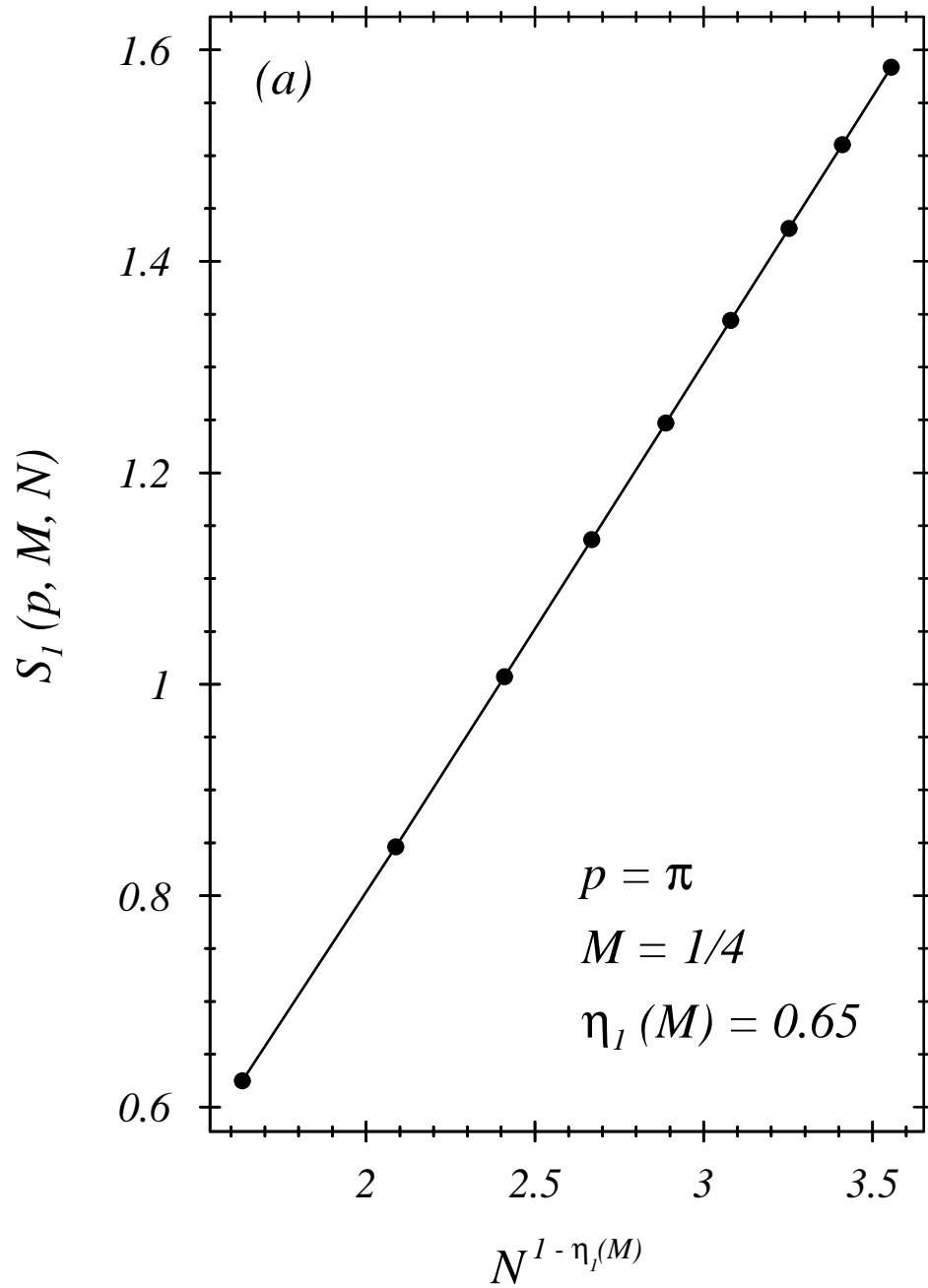


FIG.3

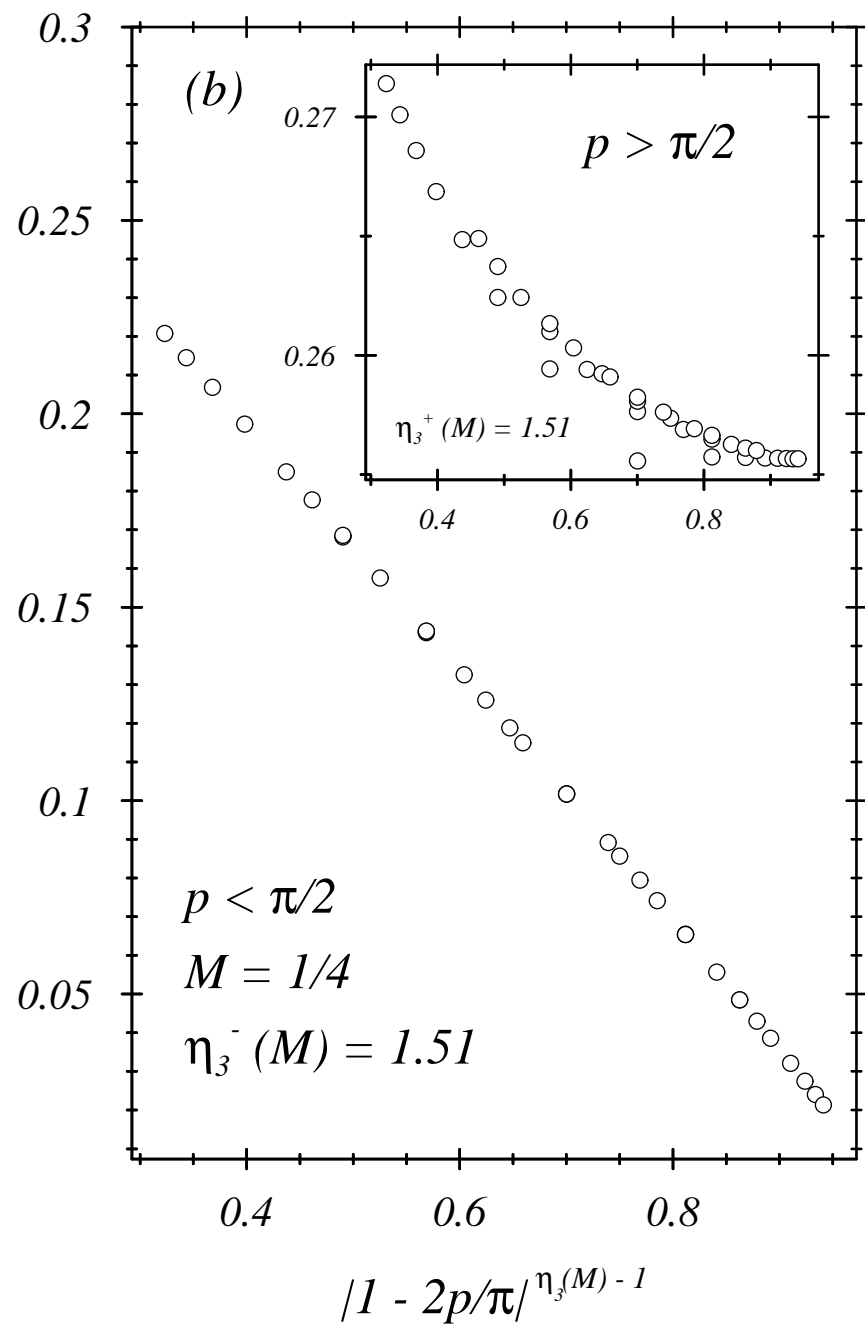
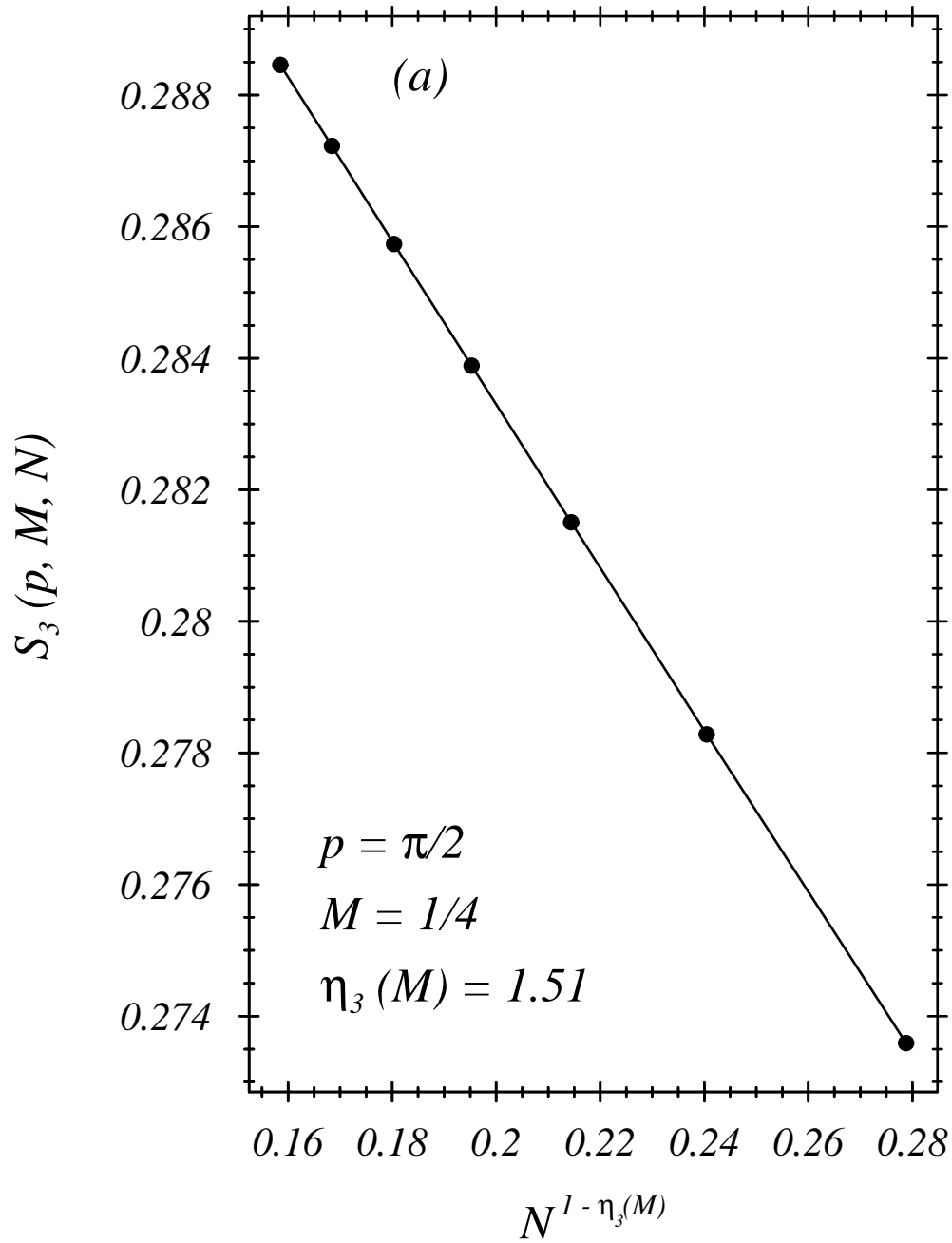


FIG.4

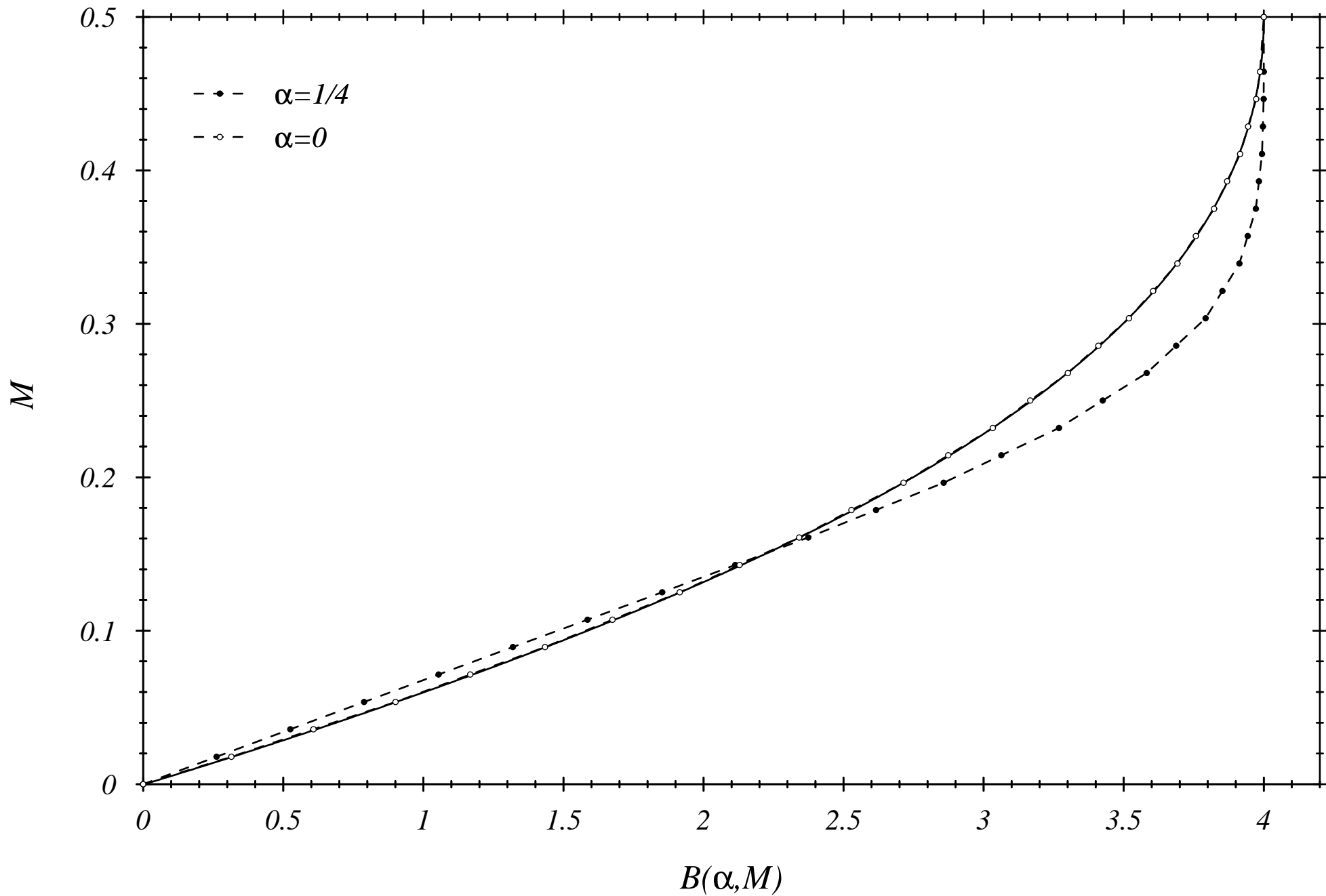


FIG.12

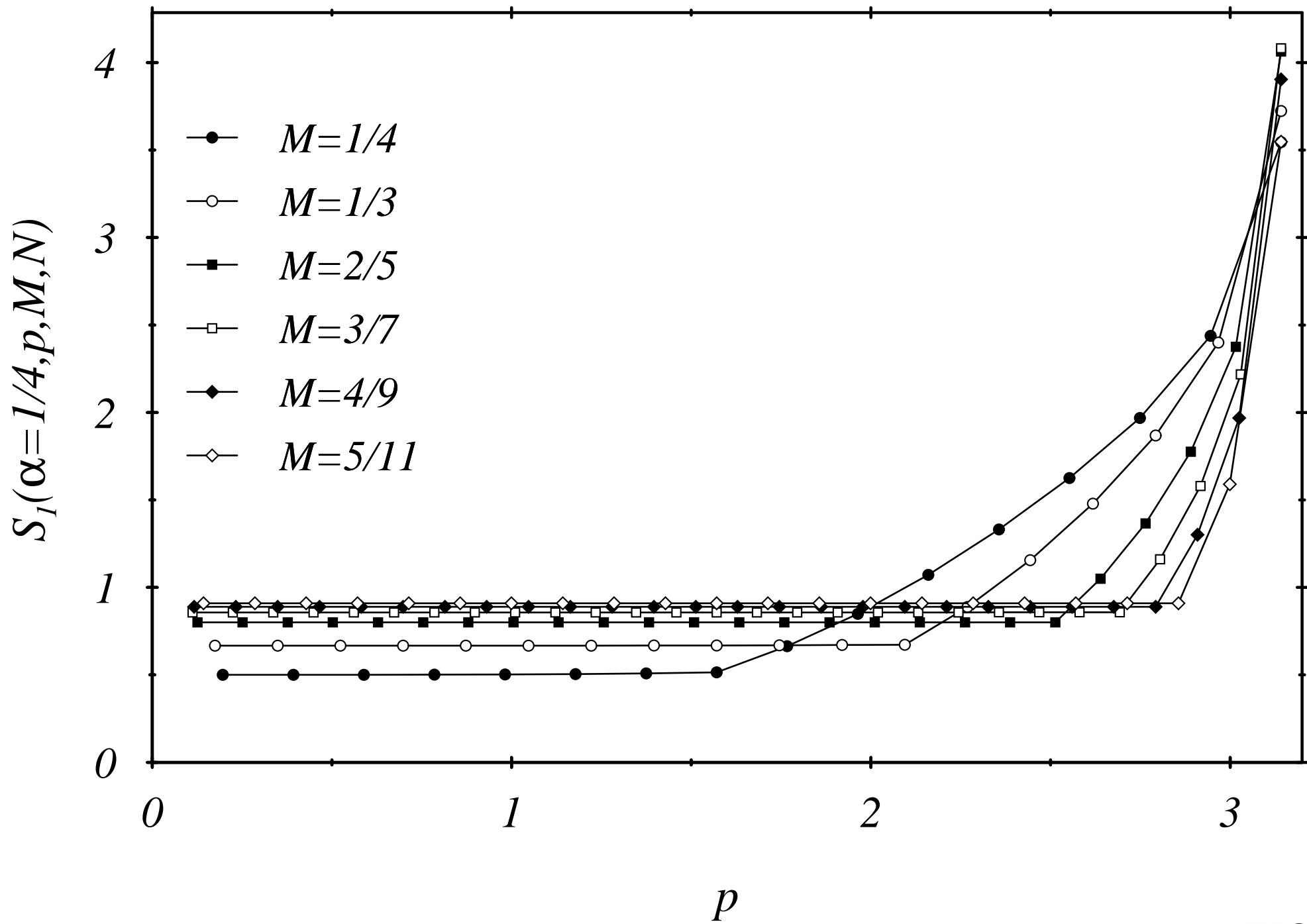


FIG.

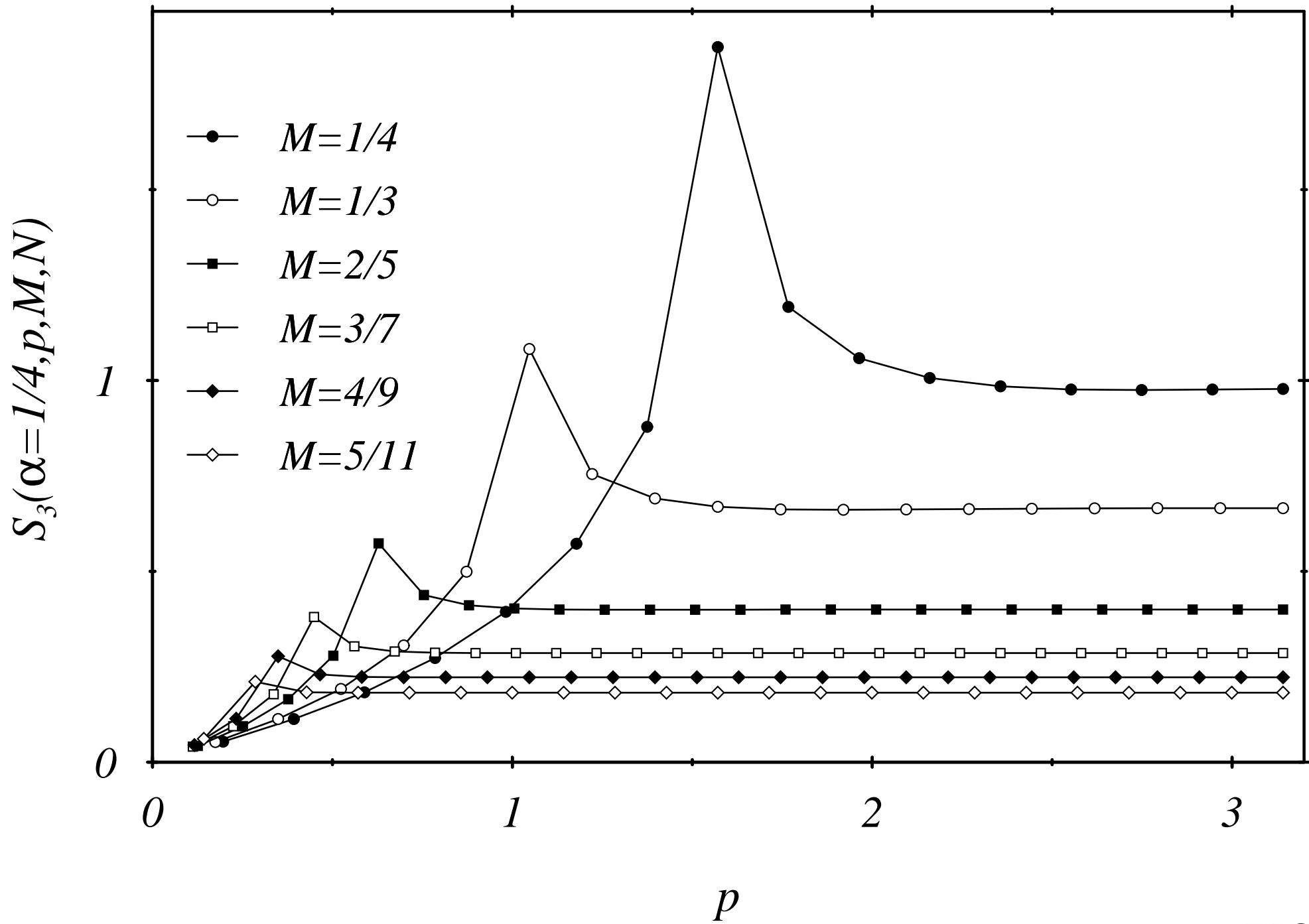


FIG.

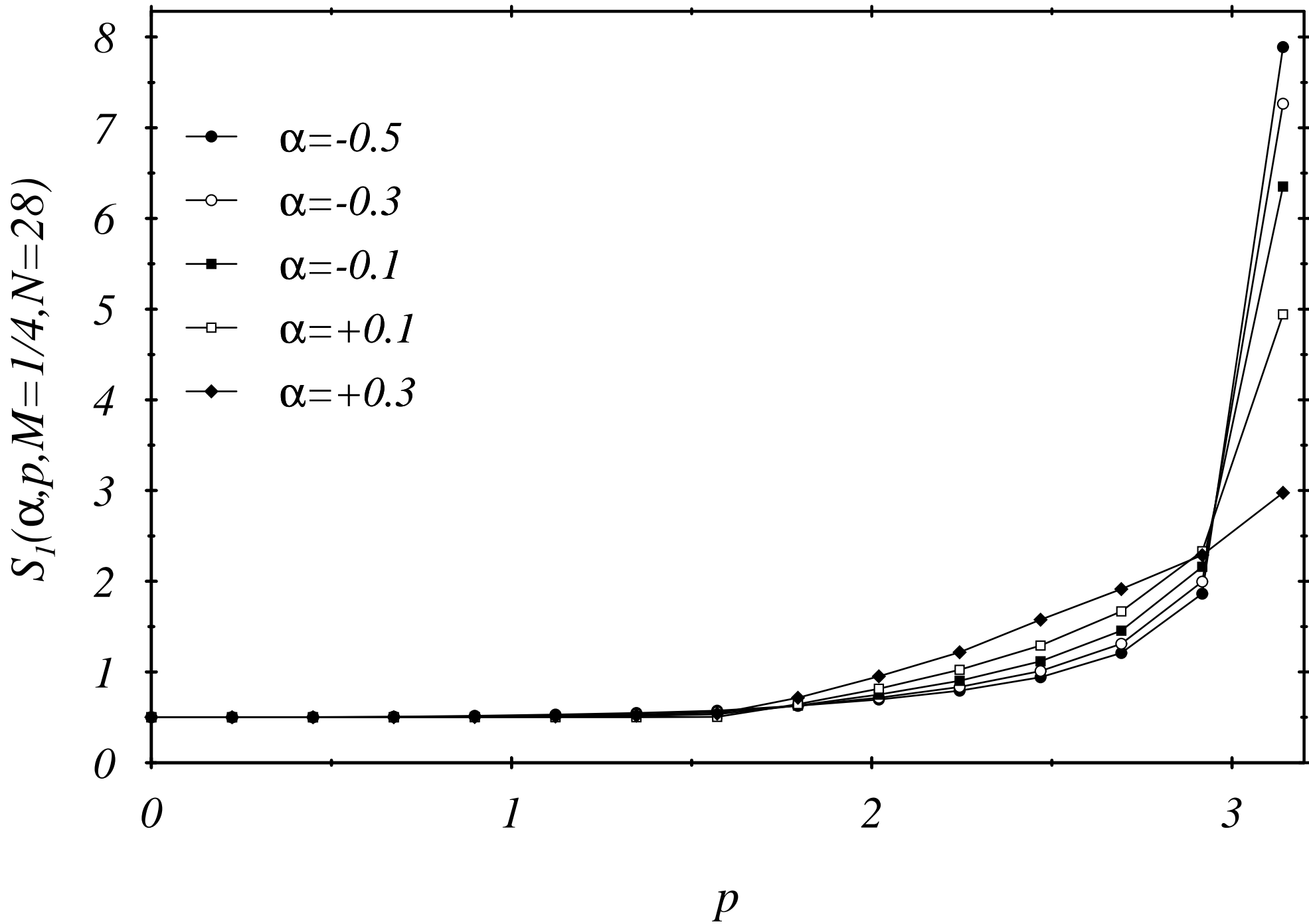


FIG.

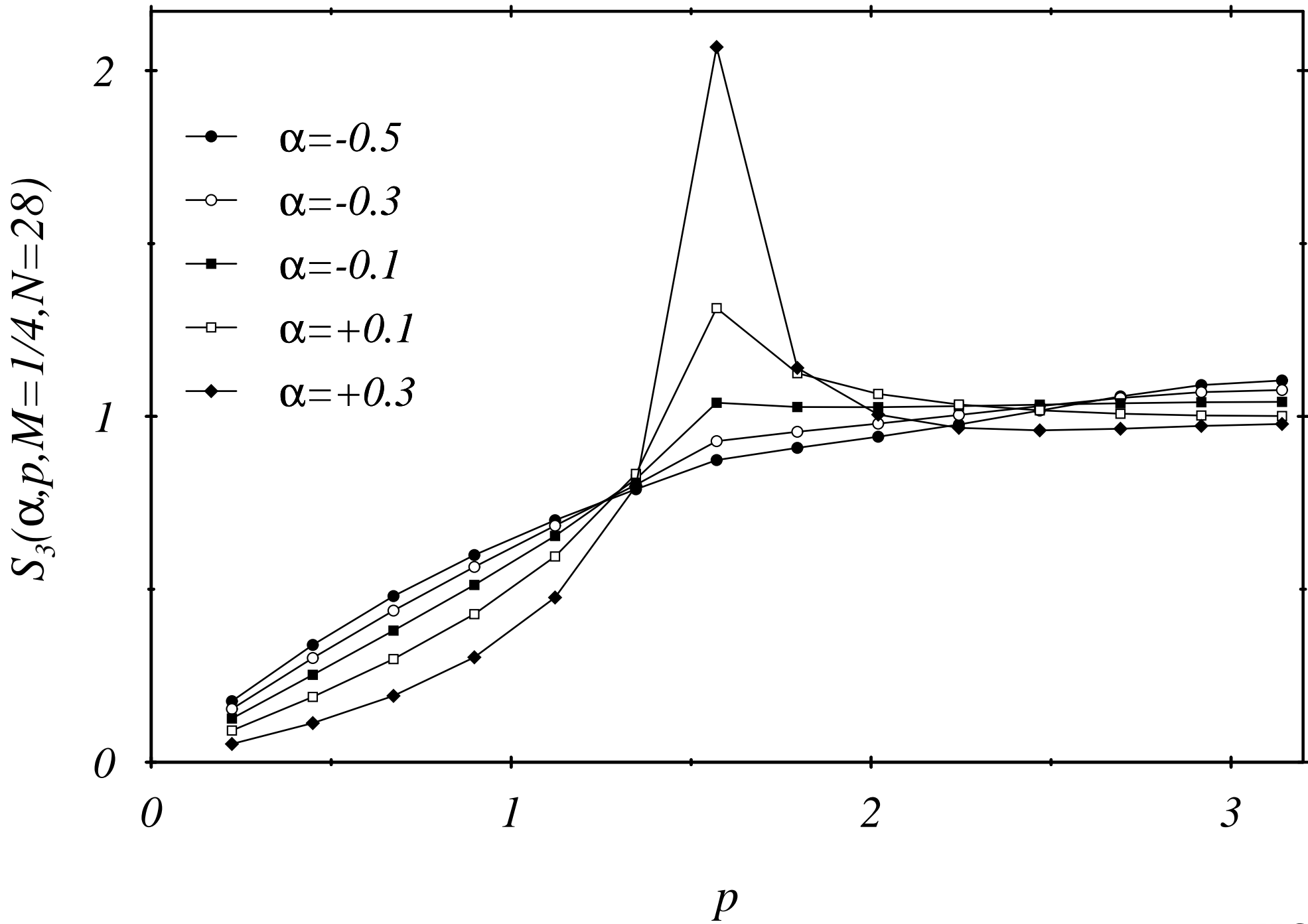


FIG.